Activation of ADF/Cofilin Mediates Attractive Growth Cone Turning Toward Nerve Growth Factor and Netrin-1

Bonnie M. Marsick,[1,2] Kevin C. Flynn,[3]* Miguel Santiago-Medina,[4] James R. Bamburg,[3,5] Paul C. Letourneau[1,2]

[1] Department of Neuroscience, University of Minnesota, Minneapolis, Minnesota 55455

[2] Graduate Program in Neuroscience, University of Minnesota, Minneapolis, Minnesota 55455

[3] Graduate Program in Cell and Molecular Biology, Colorado State University, Fort Collins, Colorado 80521

[4] Neuroscience Training Program, University of Wisconsin–Madison, Madison, Wisconsin 53706

[5] Department of Biochemistry and Molecular Biology, Colorado State University, Fort Collins, Colorado 80521

Received 29 March 2010; revised 21 April 2010; accepted 22 April 2010

ABSTRACT: **Proper neural circuitry requires that growth cones, motile tips of extending axons, respond to molecular guidance cues expressed in the developing organism. However, it is unclear how guidance cues modify the cytoskeleton to guide growth cone pathfinding. Here, we show acute treatment with two attractive guidance cues, nerve growth factor (NGF) and netrin-1, for embryonic dorsal root ganglion and temporal retinal neurons, respectively, results in increased growth cone membrane protrusion, actin polymerization, and filamentous actin (F-actin). ADF/cofilin (AC) family proteins facilitate F-actin dynamics, and we found the inactive phosphorylated form of AC is decreased in NGF- or netrin-1-treated growth cones. Directly increasing AC activity mimics addition of NGF or netrin-1 to increase growth cone protrusion and F-actin levels. Extracellular gradients of NGF, netrin-1, and a cell-permeable AC elicit attractive growth cone turning and increased F-actin barbed ends, F-actin accumulation, and active AC in growth cone regions proximal to the gradient source. Reducing AC activity blunts turning responses to NGF and netrin. Our results suggest that gradients of NGF and netrin-1 locally activate AC to promote actin polymerization and subsequent growth cone turning toward the side containing higher AC activity.** © 2010 Wiley Periodicals, Inc. Develop Neurobiol 70: 565–588, 2010

Keywords: **guidance; neurotrophins; netrin; ADF/cofilin; actin; growth cone**

INTRODUCTION

Accurate wiring of neural networks requires that axonal growth cones follow paths determined by extrinsic guidance cues (Mitchison and Kirschner, 1988; Letourneau and Cypher, 1991; Tessier-Lavigne and Goodman, 1996; Song and Poo, 1999, 2001). These cues direct growth cones by binding receptors to trigger signaling cascades that produce cytoskeletal

Additional Supporting Information may be found in the online version of this article.

**Present address:* Axon Growth and Regeneration, Max Planck Institute of Neurobiology, Martinsried, Germany.

Correspondence to: P.C. Letourneau (letou001@umn.edu).

Contract grant sponsor: NIH; contract grant numbers: EY07133, HD019950, NS40371, NS48660, NS41564.

Contract grant sponsor: Dana Foundation.

Published online 29 April 2010 in Wiley InterScience (www.interscience.wiley.com).
DOI 10.1002/dneu.20800

modifications (Theriot and Mitchison, 1991; Bentley and O'Connor, 1994; Lin et al., 1994; Tanaka and Sabry, 1995; Kozma et al., 1997; Huber et al., 2003; Lowery and Van Vactor, 2009). Despite the identification of numerous cues and signaling cascades, the roles of downstream actin regulatory proteins are poorly understood (Dent and Gertler, 2003).

Neurotrophins, which affect multiple aspects of neuronal development, are also guidance cues (Henderson, 1996; Casaccia-Bonnefil et al., 1999; Chen et al., 1999; Schuman, 1999; Davies, 2000). Studies *in vitro* (Letourneau, 1978; Gunderson and Barrett, 1979; Gunderson, 1985) and *in vivo* (Menesini Chen et al., 1978; Hassankhani et al., 1995; Patel et al., 2000; Glebova and Ginty, 2004) show that the neurotrophin nerve growth factor (NGF) is an attractive cue for sensory and sympathetic neurons and is necessary for target innervation. Netrins are another well-characterized group of guidance cues that induce attraction or repulsion depending on receptor expression (Kennedy et al., 1994; Moore et al., 2007; Round and Stein, 2007).

It is proposed that attractive cues, such as NGF and netrin-1, favor actin stabilization and polymerization in the growth cone proximal side (Seeley and Greene, 1983; Sabry et al., 1991; Lin and Forscher, 1993; O'Connor and Bentley, 1993; Gallo and Letourneau, 1997, 2000; Dent et al., 2004; Lebrand et al., 2004; Quinn et al., 2008). However, the actin-binding proteins that mediate this actin reorganization are poorly understood. Actin depolymerizing factor and cofilin (AC) family proteins remodel actin filaments by enhancing assembly/disassembly dynamics (Sarmiere and Bamburg, 2003; Andrianantoandro and Pollard, 2006; Chan et al., 2009). AC is inactivated by phosphorylation at a conserved serine3 residue by multiple kinases, including LIM kinases 1 and 2 (Arber et al., 1998; Yang et al., 1998; Toshima et al., 2001), and is activated by dephosphorylation via multiple phosphatases (Niwa et al., 2002; Endo et al., 2003; Ohta et al., 2003; Nagata-Ohashi et al., 2004; Huang et al., 2008). Furthermore, AC proteins are inhibited by phosphatidylinositol phosphates in a pH-dependent manner (Frantz et al., 2008).

Several studies suggest that AC may mediate some axonal guidance. AC proteins have roles in axon extension (Bamburg and Bray, 1987; Meberg et al., 1998; Kuhn et al., 2000; Meberg and Bamburg, 2000; Birkenfeld et al., 2001), and are implicated in regulating filopodial responses to neurotrophins (Gehler et al., 2004; Chen et al., 2006). Moreover, a direct role for AC in growth cone guidance was recently shown with X*enopus laevis* spinal neurons' response to bone morphogenic proteins (Wen et al., 2007). In carcinoma cells, AC activation stimulates local actin polymerization during chemotaxis (Ghosh et al., 2004; Mouneimne et al., 2004, 2006).

Here, we report that NGF (sensory neurons) and netrin-1 (retinal ganglion cells) stimulate plasma membrane protrusion and actin polymerization in growth cone leading margins, while increasing active AC. Direct increases in active AC also increase protrusion and growth cone F-actin levels. Local increases in active AC within the growth cone induce attractive turning, and reducing AC activity blunts turning to NGF or netrin-1. These data suggest that two important attractive cues promote growth cone turning by activating AC and inducing actin polymerization in the growth cone region proximal to the attractive cues.

METHODS

Materials

F-12 medium, B27 additives, poly-D-lysine (MW >300,000), jasplakinolide, Alexa Fluor 488 DNase1, Alexa Fluor 488- and 568-phalloidin, Alexa Fluor 488 and 568 secondary antibodies were purchased from Invitrogen. NGF, recombinant chick netrin, and L1-Fc were purchased from R & D Systems. Fc Fragment was purchased from Jackson Immuno Research. Chariot was purchased from Active Motif. White leghorn fertilized chicken eggs were purchased from Hy-Line North America, LLC. Cytochalasin D and all other reagents were purchased from Sigma-Aldrich, unless otherwise indicated.

Neuronal Culture

Glass coverslips were coated with 100 μg/mL poly-D-lysine, rinsed with water, coated with 1% nitrocellulose dissolved in 100% amyl acetate (Fischer Scientific), dried, and coated overnight with 4 μg/mL recombinant L1-Fc mixed with 8 μg/mL Fc in phosphate buffered solution (PBS; Roche). Video dishes were made by gluing a coverslip (18 mm $\times$ 18 mm; Gold Seal) over a hole (5 mm) in the bottom of a culture dish (Falcon 35 mm $\times$ 10 mm), allowed to dry, rinsed with water, and coated as described. Embryonic day 7 (E7) dorsal root ganglia (DRG) and temporal retina were removed from chick embryos according to procedures approved by the University of Minnesota Institutional Animal Care and Use Committee. Neural tissues were cultured on experimental substrates in F-12 with B27 additives and buffered to pH 7.4 with 10 m*M* HEPES. Neural tissues were cultured overnight in a humidified incubator at 37°C.

Xenopus laevis embryos were obtained as described previously (Gomez et al., 2003) and staged according to Nieuwkoop and Faber (1994). For spinal cord cultures, neural tubes were dissected from stage 22 embryos and explants were cultured in a 1$\times$ modified Ringer's solution.

Explants were plated on acid-washed glass coverslips coated with 25 μg/mL laminin (Sigma) as described previ-

ously (Gomez et al., 2003). Cultures were fixed 12–16 h after plating with 4% Paraformaldehyde in Krebs + Sucrose Fixative (4% PKS) for 15 min and rinsed with PBS.

Preparation of NGF-Coated Beads

NGF and BSA were covalently coupled to 6 μm carboxylated beads (Polysciences) as described previously (Gallo et al., 1997).

Neuronal Transfection

DRG and retinal tissue was dissociated as described by Roche et al. (2009). Approximately 2×10^6 cells were transfected with one of the following: 1 μg of plasmid co-expressing GFP and shRNA against human cofilin (control), 1 μg of a plasmid encoding the fluorescent F-actin probe, green fluorescent protein (GFP)-utrophin calponin homology domain (UtrCH) kindly provided by Dr. W. M. Bement (University of Wisconsin, Madison, WI) (Burkel et al., 2007); 2 μg constitutively active LIMK with 1 μg GFP; or 1 μg ADF shRNA using the G-13 program of the Amaxa Biosystems Nucleofector, and the chicken neuron nucleofector reagents. Cells were cultured 24–48 h, as indicated.

RNA interference (RNAi) was performed using a DNA vector to express small hairpin RNAs (shRNA) from a polymerase III promoter. Chick ADF siRNA oligonucleotides were designed using established criteria based on a corresponding sequence used successfully in mouse (Hotulainen et al., 2005; Garvalov et al., 2007) and inserted into the pSuper expression vector (Brummelkamp et al., 2002) containing the H1 polymerase III promoter. The sequence used in this study is 5′-GTGGAAGAAGGCAAAGAGATT-3′. The H1 pol III-shRNA cassette was then subcloned into pAdtrack plasmids which co-express GFP from a separate promoter, aiding the identification of transfected cells.

Time-Lapse Microscopy and Quantitative Fluorescence Determinations

A Spot digital camera mounted on an Olympus XC-70 inverted microscope, and MetaMorph software (Molecular Devices) were used for all image acquisitions. In any one experiment, all images were acquired in one session. For collection of fluorescent images, exposure time and gain settings on the digital camera were kept constant, and image acquisition and analysis was performed as described by Roche et al. (2009). In MetaMorph, a line tool was used to outline the terminal 25 μm of each distal axon and growth cone, and background intensity value was subtracted from the fluorescence intensity value of the accompanying neuronal measurement.

Video and Kymograph Analysis

E7 DRG or retinal explants were cultured 24 h, or transfected cells were cultured 48 h on L1-coated video dishes. A growth cone was selected, and imaged at 10 s intervals. When a cue reagent was added (40 ng/mL NGF or Chariot + XACA3 for DRGs, or 500 ng/mL netrin for retina), a blank frame was taken to mark the time of addition (as seen as a black line in the kymograph). The video was then opened in ImageJ and three one pixel-wide lines were drawn perpendicular to the growth cone leading edge: one in line with the neurite axis (labeled 0°), and one on either side of the 0° line, at a 30° angle (labeled −30° and 30°). The angle of the 30° lines was taken at the approximate growth cone center at the video start. Using the "stacks → reslice" function, a kymograph was generated and enlarged for better visualization.

Retrograde Flow Measurements

To determine retrograde actin flow rates, DRGs were transfected with GFP-actin, cultured overnight on L1, and imaged every 3 s for 3 min before and after the addition of 40 ng/mL NGF. Kymographs were generated for the distal 10 μm of growth cones ($n = 8$), and flow rates were measured by tracking bright GFP-actin features, which are formed by unequal incorporation of GFP- and nonGFP actin monomers into polymerized filaments at the leading edge. Measuring retrograde flow using the movement of these features has been described previously, including a demonstrated sensitivity of this retrograde flow to the myosin-II inhibitior blebbistatin (Chan and Odde, 2008).

Immunocytochemistry

Neuronal cultures were fixed and blocked as described by Roche et al. (2009). Coverslips were incubated with primary antibodies diluted in PBS containing 10% goat serum overnight at 4°C. Affinity purified antibody 12977 (ADF) was used at 1:200 dilution; 4321 (phospho-ADF/cofilin) and 3981 (XAC1) were used at 1:1000 dilution. Because both 12977 and 4321 are rabbit antibodies, we compared staining between groups of neuronal growth cones for which immunostaining and image acquisition parameters were kept identical. Coverslips were then rinsed three times in PBS and incubated in PBS rinse for 1 h. For labeling F-actin, Alexa Fluor 568-phalloidin was applied at a 1:20 dilution, and mixed with secondary antibodies: Alexa Fluor 568 goat anti-rabbit or anti-mouse antibodies at 1:1000 dilution in PBS with 10% goat serum for 1 h. For labeling G-actin, 25 ng/mL Alexa Fluor 488 DNase1 was applied to coverslips for 1 h. For staining total ADF in growth cones subjected to gradients, a pipette coated with NGF, netrin, or BSA was presented to one side of growth cones for 5 min, pipette was removed and incubated 1 min in permeabilization buffer (described below) with 100 n*M* phalloidin, fixed and stained.

Antibodies against γ-actin (7577) and β-actin pAb 2963 were generated in the lab of James Ervasti (University of Minnesota) and were kind gifts; β-actin antibody A1978 was purchased from Sigma and FITC-conjugated AC15 was purchased from Abcam. Generation of γ-actin Ab 7577

was described previously (Hanft et al., 2006) and was used at 1:100 dilution, and pAb 2963 was raised against the unique N-terminal peptide sequence of beta-actin and affinity purified against platelet actin as described by Prins et al. (2008), and was used at 1:25, For *Xenopus* and chick cultures, coverslips were incubated overnight at 4°C, rinsed in PBS, incubated 1 h in secondary. All staining, rinses, and image acquisitions were done in parallel. After rinsing three times in PBS, coverslips were mounted in *SlowFade* reagent (Invitrogen).

Pharmacological Inhibitors

Cultures were treated with 20 n*M* cytochalasin D (Invitrogen), 40 n*M* jasplakinolide, or 500 n*M* K252a (Calbiochem) for 3 min prior to NGF addition. Controls were treated with the same volume DMSO vehicle, which never exceeded 5 μL/mL.

Barbed End Labeling

This protocol was adapted from Chan et al. (1998). In summary, neurons were cultured overnight and treated as indicated. At room temp, the culture media was gently aspirated and a permeabilization buffer (1% BSA, 0.025% saponin, 138 m*M* KCL, 10 m*M* Pipes, 0.1 m*M* ATP, 3 m*M* EGTA, 4 m*M* MgCl2, pH = 6.9) with 100 n*M* Alexa-fluor 488 phalloidin (Invitrogen) was added for 1 min, after which the buffer was aspirated and buffer containing 0.45 μM Rhodamine nonmuscle actin (Cytoskeleton) was added for 4 min, after which the buffer was removed and cells were fixed with 4% paraformaldehyde and 0.05% glutaraldehyde, rinsed, and imaged.

Recombinant Proteins and Protein Loading

Recombinant XAC proteins were generated as described previously (Gehler et al., 2004). Proteins were delivered into cells using Chariot reagent (Active Motif; Morris et al., 2001), according to the manufacture's instructions. Briefly, 6 μL Chariot was complexed with 1 μg BSA, XACWT, or XACA3 for 1 h, then added to the culture medium or immobilized onto a nitrocellulose-coated micropipette.

Growth Cone Turning Assay

Turning was assessed as described previously (Roche et al., 2009). Briefly, micropipette tips were dipped in a 1% nitrocellulose solution, dried, then dipped several times in a PBS solution of 1 μg/mL NGF, BSA, XACA3, Chariot + XACA3, Chariot + BSA, or 10 μg/mL netrin (retina). A growth cone was imaged at 30 or 60 s intervals for 15 min. The micropipette tip was then positioned 100 μm from a growth cone at a 45° angle to the direction of axon elongation. Images were acquired 45 min after introducing the micropipette tip. NGF or Chariot + XACA3 was added to the culture medium at the beginning of some of the videos. Growth cone turning angles were determined as the change in direction of growth cone migration between the beginning and end of the image acquisition period (Ming et al., 1997).

Effects of Chariot-A3 Gradient on GFP-UtrCH Distribution in DRG Growth Cones

This was performed as described previously by Roche et al. (2009).

Statistical Analysis

Parameters of population values are reported as Mean ± SEM. All statistical analysis was by unpaired Student's *t* test, Mann-Whitney *U* test, or ANOVA for multiple comparisons.

RESULTS

Nerve Growth Factor and Netrin-1 Induce Growth Cone Leading Edge Protrusion

Guidance cues regulate growth cone motility. To assess the effects of attractive cues on protrusive activity, we cultured embryonic day 7 (E7) chick dorsal root ganglion (DRG) or temporal retina explants overnight on L1CAM, then imaged growth cones at 10 s intervals for 5 min before and 5 min after adding 40 ng/mL NGF (for DRGs) or 500 ng/mL netrin (for retina) to the medium (Lebrand et al., 2004). We then generated kymographs of motility at three locations at the growth cone leading edge, in line with the neurite axis (0°) and at 30° to either side of the axis (−30° and 30°). As seen in the kymographs, membrane protrusion from DRG and retinal growth cones increased within seconds of guidance cue addition [Fig. 1(A,B)].

To better quantify this membrane protrusion we plotted the leading edge position in pixel numbers relative to the time of cue addition. These spatial positions were then averaged across five growth cones for each condition. As shown in Figure 1(C,D), membrane protrusion is stimulated at all three kymograph locations at the growth cone leading edge following NGF or netrin addition.

Nerve Growth Factor and Netrin-1 Increase Growth Cone F-Actin and Free Barbed Ends

As growth cone membrane dynamics depend on the underlying actin cytoskeleton, we next examined the

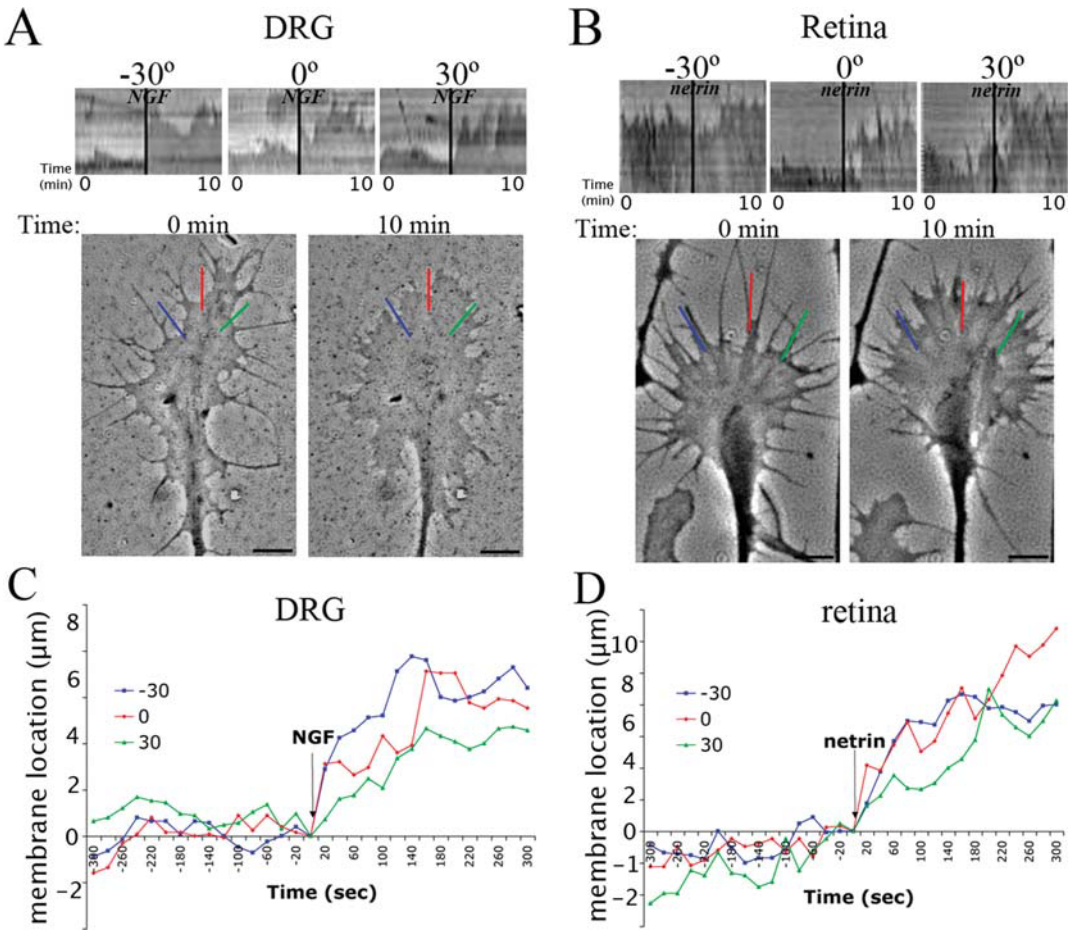

Figure 1 Nerve growth factor and netrin-1 induce leading edge protrusion. Embryonic day 7 (E7) DRG (A and C) or temporal retinal explants (B and D) were cultured overnight on L1CAM. A growth cone was imaged every 10 s for 5 min before and after adding 40 ng/mL NGF (A) or 500 ng/mL netrin-1 (B). Kymographs at three locations were generated using a line perpendicular to growth cone leading edge: one in line with the neurite axis (0°) and 30° to either side (−30° and 30°). In panels C and D, kymographs were quantified to track position of the leading edge before and after addition of NGF (C) or netrin (D), and averaged across five growth cones per condition. Scale bars: 10 μm. [Color figure can be viewed in the online issue, which is available at www.interscience.wiley.com.]

changes in actin organization that accompany this increased membrane protrusion. We visualized monomeric actin (G-actin), using fluorescein-conjugated DNase I (Barak et al., 1981), and fluorescent phalloidin-stained filamentous actin (F-actin) in growth cones treated with control media, NGF (DRG), or netrin (retina). This method was validated using cytochalasin D and jasplakinolide, agents that prevent and promote actin polymerization, respectively (Fig. S1). Fluorescence intensities were quantified by tracing growth cones, subtracting background, and determining the mean growth cone integrated pixel intensity. Compared to controls, DRG growth cones treated with NGF for 5 min had a relative decrease in G-actin and increase in phalloidin-stained F-actin [Fig. 2(A,C)]. Similar changes were seen in temporal retina growth cones treated 5 min with netrin [Fig. 2(B,D)]. These data show an increased ratio of phalloidin to DNase I labeling (for DRGs, −NGF = 0.85 ± 0.07, +NGF = 2.38 ± 0.37; for retina, −netrin = 3.96 ± 0.42, +netrin = 8.42 ± 1.70), suggesting a shift from G-actin to F-actin in growth cones responding to NGF or netrin.

An increase in F-actin could result from decreased actin filament depolymerization and/or an increase in actin polymerization. To assess the number of F-actin barbed ends available for polymerization, we adapted a method for the first time to primary neurons in which cells are briefly permeabilized with saponin and then rhodamine-actin is added to polymerize the

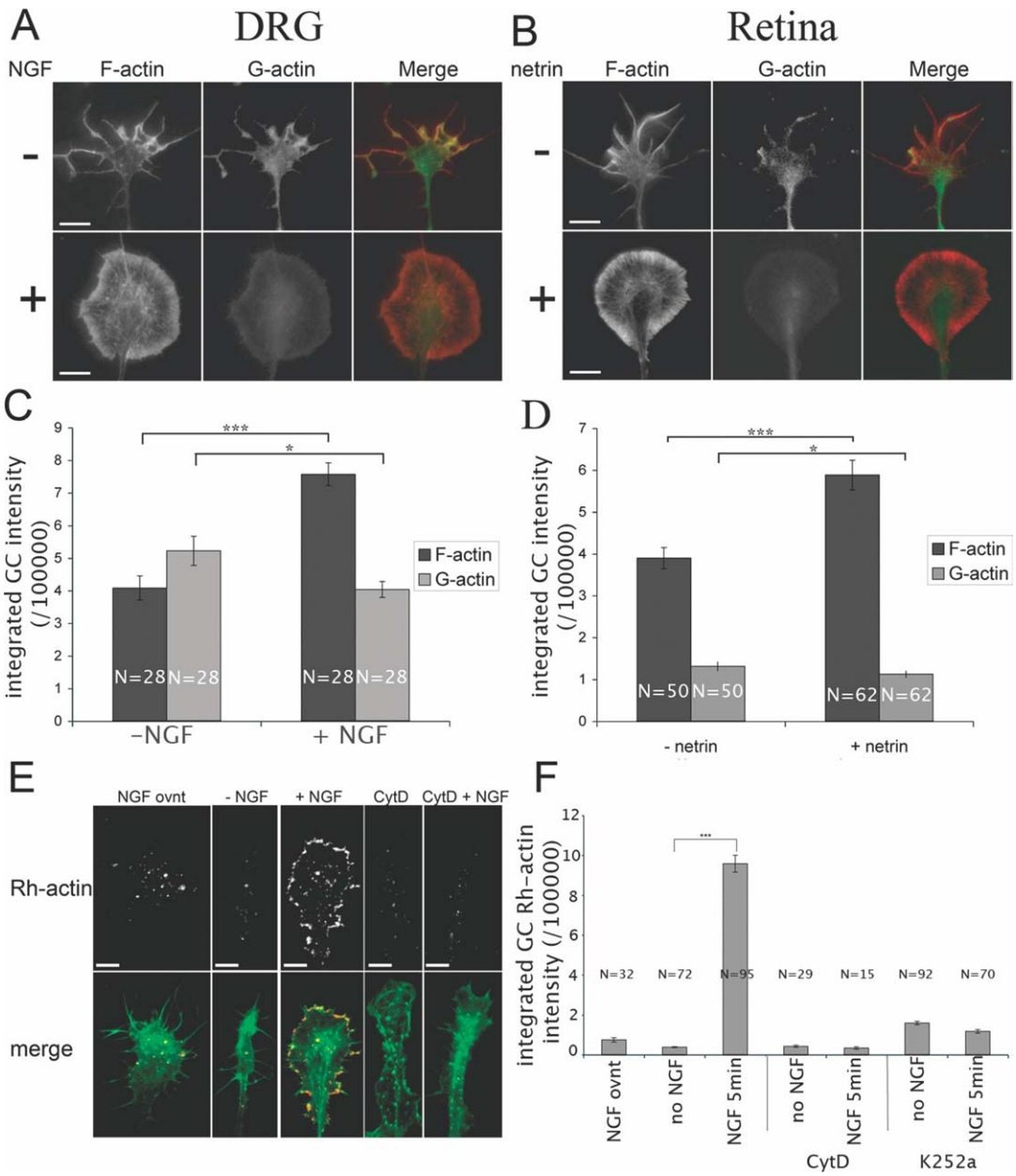

Figure 2 Nerve growth factor and netrin-1 increase growth cone F-actin, and NGF increases free F-actin barbed ends. DRG (A and C) or retinal explants (B and D) were treated 10 min with 40 ng/mL NGF (A) or 500 ng/mL netrin (B), then fixed. Quantitative fluorescence measurements of growth cone F-actin (Alexa Fluor 568-phalloidin; red) and G-actin (fluorescein-conjugated DNase1; green) were performed. Panels C and D show integrated growth cone (GC) fluorescence intensity of F-actin and G-actin in experimental populations. Panel E shows DRG growth cones stained to label F-actin (Alexa Fluor 488-phalloidin, green) or free actin barbed ends (Rh-actin, red). Panel F shows integrated rhodamine-actin growth cone intensity. Statistical significance using Student's *t* test. Data are Means ± SEM; $*p < 0.05$; $***p < 0.0001$. Scale bars: 10 μm.

free F-actin barbed ends (Chan et al., 1998). DRG growth cones treated 15 min with 40 ng/mL NGF before permeabilization showed significantly more rhodamine-actin addition to free F-actin barbed ends at the leading edge compared to growth cones of neurons treated with medium alone or grown overnight in 40 ng/mL NGF [Fig. 2(E,F)]. Both cytochalasin D (20 n*M*), which caps barbed ends, and K252a

(500 n*M*), an inhibitor of Trk receptors, blocked the NGF-induced increase in F-actin barbed ends available for rhodamin-actin.

The amount of F-actin at the leading growth cone margin is increased by actin polymerization and decreased by retrograde actin transport. Thus, a decrease in retrograde actin flow might contribute to the net F-actin increase that is induced by NGF. We, therefore, measured retrograde flow at growth cone leading margins by tracking the movement of bright F-actin features in kymographs of DRG neurons transfected to express GFP-actin (Chan and Odde, 2008). We found that retrograde actin flow was not significantly different after adding 40 ng/mL NGF (10.5 ± 0.6 μm/min; $n = 9$) than before NGF addition (11.4 ± 0.5 μm/min; $n = 9$) (Fig. S2). Together, these data suggest that NGF and netrin increase F-actin levels in DRG and retinal growth cones, respectively, by stimulating F-actin polymerization.

Gradients of Nerve Growth Factor and Netrin-1 Locally Increase F-Actin and Free Barbed Ends

We next tested whether an increase in F-actin occurs locally in growth cones encountering extracellular gradients of NGF and netrin. Gradients were created by coating a micropipette tip with a protein solution and then placing the pipette tip near a growth cone (Roche et al., 2009). Figure S3(A) shows that a gradient of rhodamine-BSA was rapidly released from a nitrocellulose-coated micropipette tip, was established at 1 min, was sustained at 5, 15, and 15 min, and extended beyond the 100 μm distance from the pipette tip to a theoretical growth cone. Producing gradients this way, DRG growth cones turn toward an NGF source [Fig. 3(A), 7(B), and 8(B)] and retinal growth cones turn toward a netrin source [Fig. 8(C); Movie S1].

To assess the effects of guidance cue gradients on growth cone F-actin distribution we fixed growth cones 5 min after the introduction of BSA-, NGF-(DRG), or netrin-(retina) coated micropipettes, then labeled F-actin with fluorescent phalloidin. To quantify asymmetries in F-actin distribution, we measured the integrated phalloidin intensity in 20×20 pixel-wide boxes in three regions across the growth cone width, and calculated the distal (region1/region2) and proximal (region3/region2) intensity ratios relative to the center [Fig. 3(B)]. Pseudo-colored images of fluorescent phalloidin staining intensity in growth cones indicated that F-actin content is higher in growth cone sides proximal to an NGF (DRG) or netrin (retina) source, but this asymmetry was not present in growth cones exposed to a BSA gradient [Fig. 3(C)]. Quantification of this phalloidin staining further indicated higher F-actin levels in regions proximal to the NGF or netrin source, but not a BSA source [Fig. 3(D)]. These data support the hypothesis that netrin and NGF gradients induce increased F-actin in growth cone regions closer to the attractive cue source.

To determine if local increases in free F-actin barbed ends also occur, we performed our barbed end labeling assay on growth cones subjected to a NGF (DRG) or netrin (retina) gradient for 5 min. Growth cones from DRGs had increased barbed ends proximal to the NGF source, where no such asymmetry occurred with a BSA gradient [Fig. 3(E)]. A similar increase was also found in retinal growth cones subjected to a netrin gradient. Because recent studies in *Xenopus laevis* growth cones have shown local protein synthesis plays a role in growth cone guidance (Leung et al., 2006; Yao et al., 2006), we bath-applied the protein synthesis inhibitor cycloheximide at 20 μM (see image in panel E) five minutes prior to introduction of the NGF gradient, and found this local increase in F-actin barbed ends still occurred. The majority of barbed end labeling was at the leading edge, so to quantify the distribution we traced a 5 pixel-wide line from the distal base of the growth cone along the leading margin to the proximal base, and obtained an intensity profile [Fig. 3(E)]. This intensity line was then divided, and the pixel intensities along the line segments proximal and distal to the cue were summed. We found the proximal/distal ratio of barbed end staining intensity was significantly higher in DRG growth cones exposed to an NGF gradient versus a BSA gradient [Fig. 3(E)]. Together, these data suggest NGF (DRG) and netrin (retina) locally stimulate actin polymerization proximal to the cue source.

ADF/Cofilin Family Proteins are Activated by NGF and Netrin

We next investigated the role of AC family proteins in this guidance cue-induced F-actin increase. AC proteins are inactivated by phosphorylation at serine 3. Upon dephosphorylation, AC proteins bind to and modify actin filaments. To determine if acute NGF addition affects the level of active AC, we measured the levels of total chick ADF and inactive phosphorylated ADF/cofilin (pAC) in growth cones via immunocytochemistry, using FITC as a control for total protein. Previous work has shown that expres-

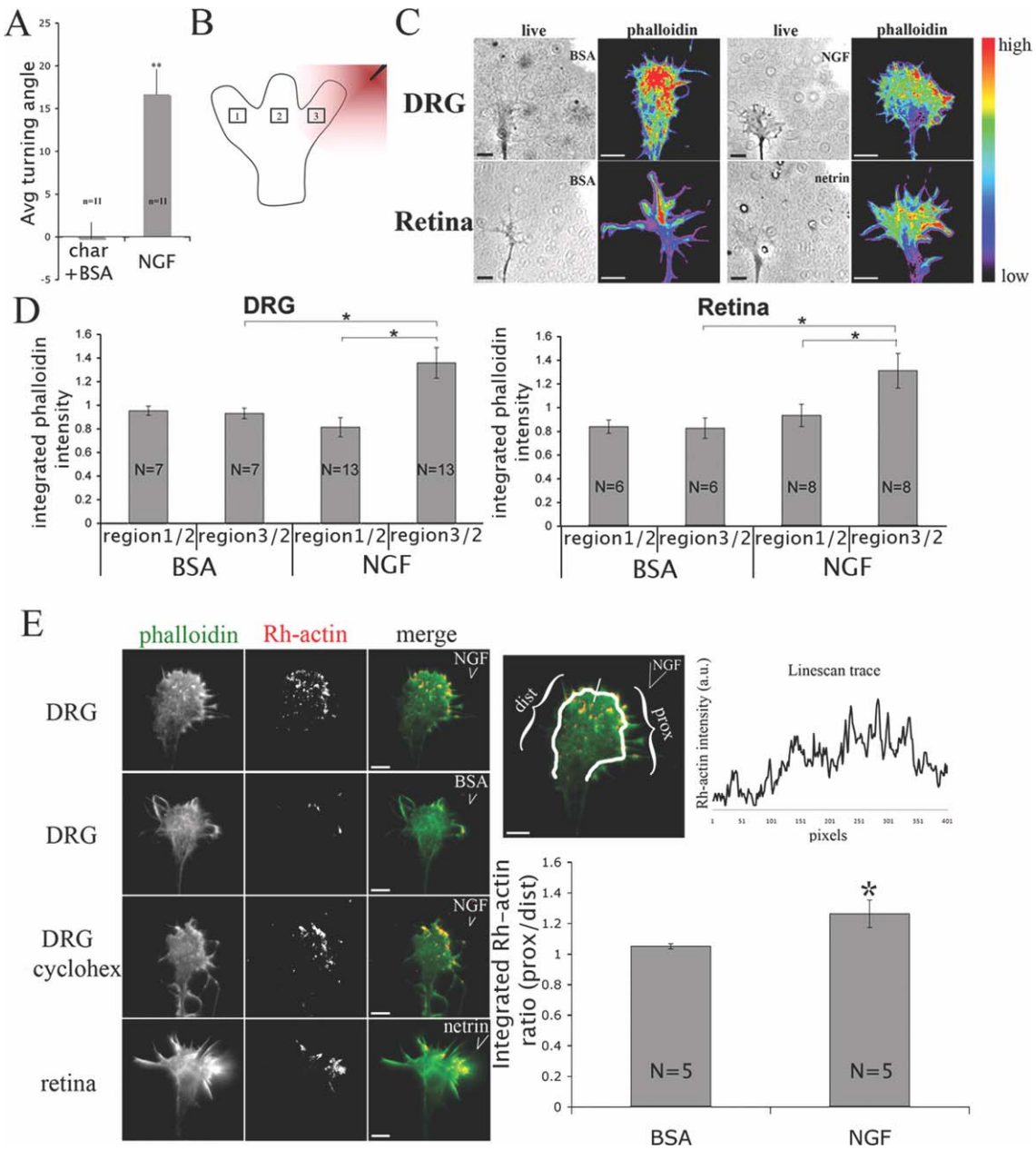

Figure 3 Growth cones exposed to a gradient of NGF or netrin-1 exhibit asymmetrical F-actin free barbed end distribution. DRG growth cones turn toward NGF (A), data is taken from panel 7B of this article. Panel B depicts method used to quantify F-actin (in 3C, D, 6B) distribution across growth cones by measuring integrated intensities in 20 × 20 pixel-wide regions. Micropipette releasing protein is located to the right side of growth cones. For panel C, a micropipette releasing BSA, NGF, or netrin is introduced to one side of a DRG or retinal growth cone for 5 min, fixed, stained for F-actin (Alexa-488 phalloidin), and pseudo-colored. Distribution was quantified by taking the integrated intensities proximally (region 3) and distally (region 1), relative to the growth cone center (region 2). Panel E shows phalloidin (green) and barbed end (red) labeling on growth cones subjected to a gradient of NGF (DRG), netrin (retina), or BSA for 5 min. Barbed end labeling distribution was performed taking the Rh-actin intensity linescan along growth cone membrane border, dividing in half, and computing the integrated ratio of proximal/distal intensity. Statistical significance using Student's *t* test. Data are Means ± SEM; $*p < 0.05$; $**p < 0.001$. Scale bars: 10 μm.

sion of ADF in chick brain greatly exceeds (about 10-fold) expression of cofilin (Devineni et al., 1999). Compared to untreated growth cones, 5 min treatment with NGF had no significant effect on the total amount of ADF in growth cones, but did significantly lower the total levels of phospho-AC [Fig. 4(A)]. Similarly, 5 min treatment of retinal neurons with netrin significantly reduced total phospho-AC levels but not total ADF [Fig. 4(B)].

Having found that global addition of NGF reduces the content of inactive phospho-AC in DRG growth cones, we wanted to know if a local NGF source stimulates local AC activation. To do so, we examined the levels of phospho-AC in regions of growth cones that touched a bead with surface-bound NGF (Gallo and Letourneau, 1998, 2004). DRG cultures were incubated with 6 μm beads conjugated with BSA or NGF for 60 min, then fixed and stained for phospho-AC, FITC (total protein), and fluorescent phalloidin binding (F-actin). Compared to growth cone regions that contacted a BSA bead or growth cone regions that did not contact NGF- or BSA-beads, there was a significantly lower phospho-AC level in growth cone regions that contacted an NGF bead [Fig. 4(C)].

Despite the above demonstrations that phospho-AC levels are reduced by global NGF or netrin and reduced near contact with NGF-coupled beads, we were not able to detect local phospho-AC staining differences in growth cones exposed to gradients of NGF or netrin. Several reasons may account for this. Compared to conditions where small growth cone regions were contacting a local and stable NGF source presented on a bead [Fig. 4(C)], the gradient of NGF across the growth cone width using the micropipette is comparatively shallow. Furthermore, the fixation of a relatively small (20 kDa) and soluble protein such as phospho-AC, which does not bind F-actin, may not be rapid enough to preserve its distribution in this shallow gradient, and these small differences may be undetectable using our immunocytochemical methods. Although Wen et al. (2007) demonstrated asymmetric phospho-AC distribution in *Xenopus* growth cones responding to BMPs, these growth cones turned away from regions of higher AC activity, suggesting the gradient of pAC may be steeper in this repulsion behavior compared to a growth cone turning toward higher AC activity. Furthermore, *Xenopus* growth cones have less actin compared to our chick growth cones (see Fig. 10), which suggests differences in actin regulation exist between the two species.

However, the asymmetric labeling of barbed ends in this gradient [Fig. 3(E)] suggests asymmetric AC activation does occur. Thus, to probe localized AC activity in our conditions used for growth cone turning, we exposed growth cones to a NGF or netrin gradient for 5 min, and applied our phalloidin-containing permeabilization buffer for 1 min prior to fixation. Under these conditions, all phospho-AC staining was lost, presumably because inactive phospho-AC is not bound to F-actin and diffuses from the growth cone upon permeabilization. We then stained for total ADF, assuming that active ADF would be bound to F-actin, and not lost upon permeabilization. Under these conditions, we found significantly higher ADF staining proximal to the NGF (DRG) or netrin (retina) source, with no such asymmetry in growth cones exposed to a gradient of BSA [Fig. 4(D)]. Together, these data suggest that NGF and netrin activate AC in DRG and retinal growth cones, respectively, in both a global and localized manner.

Increased AC Activity Results in Increased F-Actin and Barbed Ends

Results thus far suggest that increased AC activity contributes to the NGF- and netrin-1—induced increase in growth cone F-actin. To test this, we used the Chariot reagent, which forms cell-permeable complexes with proteins, to load purified recombinant *Xenopus* ADF/cofilin into our cultured neurons. Chariot-mediated incorporation of these proteins into growth cones was confirmed immunocytochemically, using an antibody against *Xenopus* AC (XAC1) that has little cross-reactivity with chick AC (Shaw et al., 2004). Compared to chick DRGs incubated 1 h with Chariot alone or wild-type *Xenopus* AC (XACWT) not complexed with Chariot, growth cones treated with Chariot-XACWT had significantly more XAC1 staining [Fig. 5(A)]. Thus, using this method we loaded DRG and retinal neurons with Chariot complexes of XACWT or a "constitutively active" XAC with a serine3 to alanine mutation that renders it non-phosphorylatable (XACA3; Gehler et al., 2004). We assessed G- and F-actin levels as before, and found in both neuronal types that the Chariot-mediated incorporation of XACWT or XACA3 increased phalloidin-stained F-actin levels and reduced DNase I staining of G-actin [Fig. 5(B,C)]. The addition of NGF to XAC-loaded DRG growth cones further increased F-actin levels, presumably through activation of endogenous AC. Netrin addition to XAC-loaded retinal growth cones did not significantly alter F-actin levels, which could be due to actin properties in retinal growth cones that limit the extent of F-actin increase upon XAC-loading and netrin addition. In

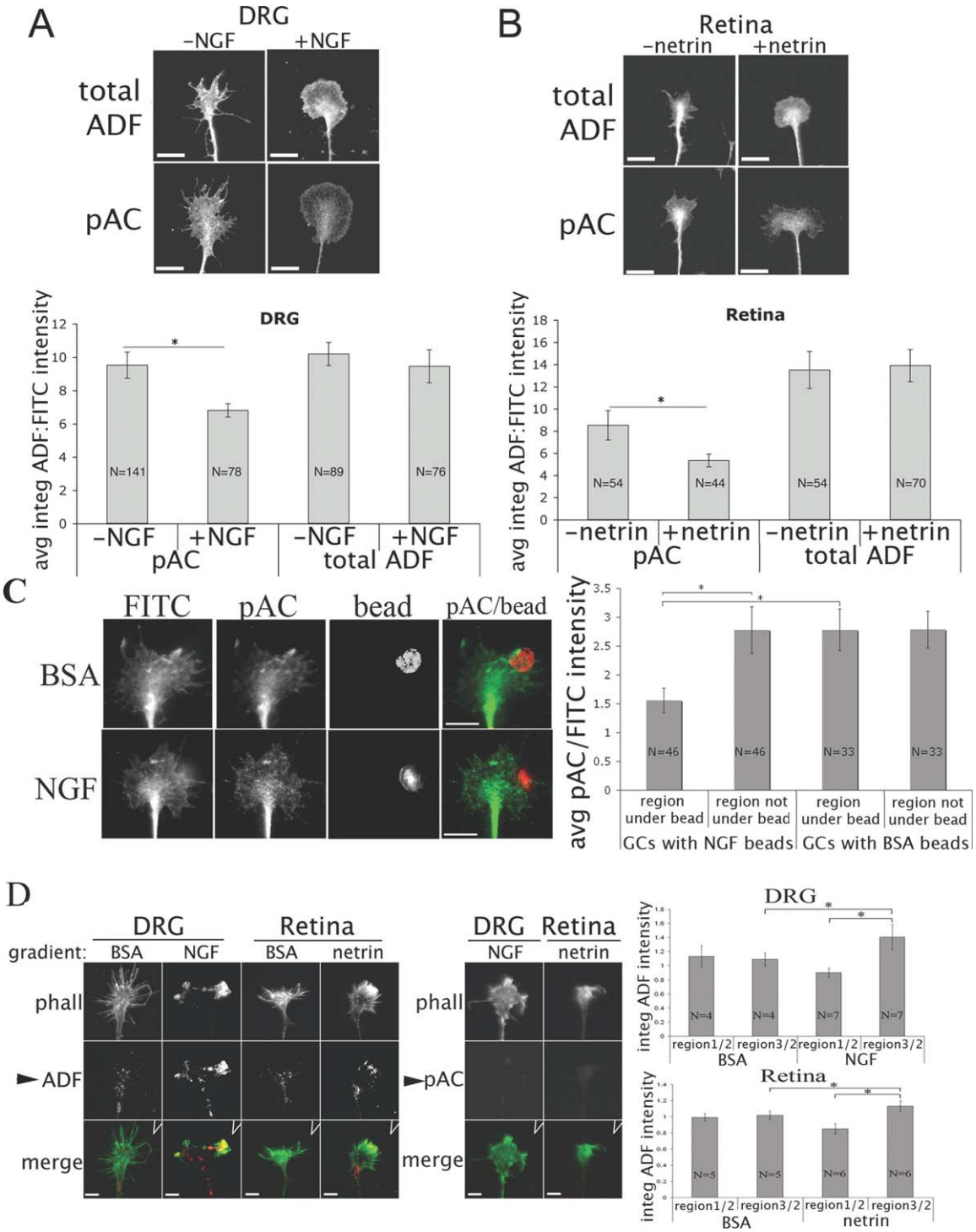

Figure 4 ADF/cofilin family proteins are activated by NGF and netrin-1. DRG (A) or retinal explants (B) were treated with medium or 40 ng/mL NGF (A) or 500 ng/mL netrin-1 (B) for 5 min, fixed and stained for chick ADF (ab 12977) or phospho-ADF/cofilin (pAC; ab 4321), and FITC (total protein). Mean growth cone integrated (avg integ) intensity values were normalized to FITC. Panel C shows DRG growth cones incubated with BSA- or NGF-conjugated beads (pseudo-colored red from phase image) for 1 h, fixed, and stained for total protein (FITC), and pAC (green). Average intensities shown for growth cone regions under BSA or NGF beads, as well as regions of the same growth cone not under a bead, and normalized to FITC. Panel D shows pAC and total ADF (ab 12977) staining after growth cones were subjected to a NGF (DRG), netrin (retina), or BSA gradient for 5 min, permeabilized for 1 min with phalloidin, then fixed and stained. Quantifications were performed as in Figure 3(B), and experiments were done on 3 separate days. Statistical significance using ANOVA. Data are Means ± SEM; $*p < 0.05$. Scale bars: 10 μm.

support of this, the magnitude of XAC-induced F-actin increase in retinal neurons was smaller compared to DRGs. Taken together, these data demonstrate that directly elevating AC activity increases F-actin in DRG and retinal growth cones.

Because the severing activity of AC proteins can increase the number of F-actin barbed ends available for polymerization, we assessed if incorporation of AC into growth cones increases F-actin barbed ends. We treated DRG growth cones 1 h with Chariot alone or Chariot complexed with XACWT or XACA3 and then assayed for F-actin barbed ends. Compared to controls, XACWT- or XACA3-treated growth cones had significantly higher levels of free barbed ends [Fig. 5(D)]. In addition, NGF treatment of XACWT- or XACA3-treated neurons further increased barbed end labeling, likely due to activation of endogenous chick AC. In addition, the morphology of NGF-treated growth cones was larger and more flattened than growth cones incubated with Chariot-XAC alone [Fig. 5(D)], suggesting that NGF induces additional changes that contribute to the change in growth cone shape.

Taken together, these data show that direct elevation of active AC increases F-actin levels in DRG and retinal growth cones, mimicking the effects seen with NGF and netrin. Furthermore, the direct elevation of AC also increases F-actin barbed ends in DRG growth cones.

Gradients of Cell-Permeable Active AC Induce Local Increases in F-Actin and Attractive Growth Cone Turning

Our data show global and local addition of the guidance cues NGF and netrin increase growth cone F-actin and AC activity, and directly increasing AC activity also increases growth cone F-actin. We next examined growth cone turning behavior, F-actin distribution and AC asymmetry in growth cones responding to gradients of cell-permeable Chariot-XACA3. Figure S3(B) shows that Chariot-rhodamine-BSA complexes diffused similarly from micropipette tips as rhodamine-BSA [Fig. S2(A)]. Gradients of Chariot-XACA3 induced attractive turning of both DRG and retinal growth cones [Fig. 7(A), Movies S2 and S3], while growth cones did not turn in a Chariot-BSA gradient [Fig. 7(B)]. Importantly, growth cones also did not turn in a gradient of extracellular XACA3 that was not complexed with Chariot, indicating that growth cone turning is induced by an intracellular, but not extracellular, asymmetry of AC activity. To show that this method does produce an intracellular asymmetry in XAC, we fixed growth cones 15 min after introduction of a micropipette coated with Chariot-XACWT or XACWT alone, then stained the growth cones with an antibody selective for *Xenopus* AC (XAC1). Quantification of growth cone XAC1 staining distribution showed that growth cones exposed to a gradient of XACWT without Chariot had no asymmetry in XAC1 staining, whereas growth cones subjected to a Chariot-XACWT gradient had higher XAC1 staining proximal to the micropipette [Fig. 6(A)]. These results indicate that growth cones turn toward the side with higher intracellular AC activity. To determine if this local increase was associated with locally increased F-actin, DRG growth cones were subjected to pipette tips coated with Chariot-XACA3 or XACA3 alone for 15 min, fixed and then stained with fluorescent phalloidin. Similar to our results with an NGF or a netrin gradient, fluorescent phalloidin staining was more intense in the growth cone regions proximal to a Chariot-XACA3 source but not a source of XACA3 alone [Fig. 6(B)].

F-actin distribution in live cells can be visualized by transfection to express an F-actin binding domain of utrophin conjugated to GFP (GFP-UtrCH; Burkel et al., 2007). To examine F-actin distribution in real time we transfected DRG neurons with GFP-UtrCH, and as reported by Roche et al. (2009), the GFP-UtrCH fluorescence intensity was higher in the proximal side of growth cones at 2 min after introducing an NGF gradient (6C; Roche et al., 2009). A BSA gradient produced no asymmetry in the distribution of GFP-UtrCH intensity. We used this approach to confirm results based on phalloidin staining that F-actin is more concentrated in the growth cone region proximal to a chariot-XACA3-releasing pipette tip [Fig. 6(B)]. DRG neurons were transfected to express GFP-UtrCH, and we assessed F-actin distribution in live growth cones that were subjected to a gradient of Chariot-XACA3. A fluorescence image was taken before and 5 min after introducing a Chariot-XACA3-coated pipette tip to one side of a growth cone. To analyze the response, a 15 pixel wide line was drawn across a growth cone and the "linescan" function was used to generate fluorescence intensity measurements across the growth cone width (in Metamorph). To quantify GFP-UtrCH distribution, the proximal/distal intensity ratios of growth cones before and after introducing the pipette were computed. For GFP-UtrCH expressing growth cones exposed to a Chariot-BSA gradient, this ratio was 1.12 ± 0.05 SE ($n = 9$), and for growth cones exposed to Chariot-XACA3 the ratio was 1.40 ± 0.09 ($n = 10$), which was significantly different from

growth cones exposed to Chariot-BSA ($p < 0.05$) [Fig. 6(C)]. As a control for volumetric changes after introducing the Chariot-XACA3 gradient, we measured fluorescence intensity across GFP only transfected growth cones. The proximal/distal GFP ratio of 0.90 ± 0.09 ($n = 8$) was not significantly different from GFP-UtrCH transfected growth cones exposed to a Chariot-BSA gradient, suggesting that the

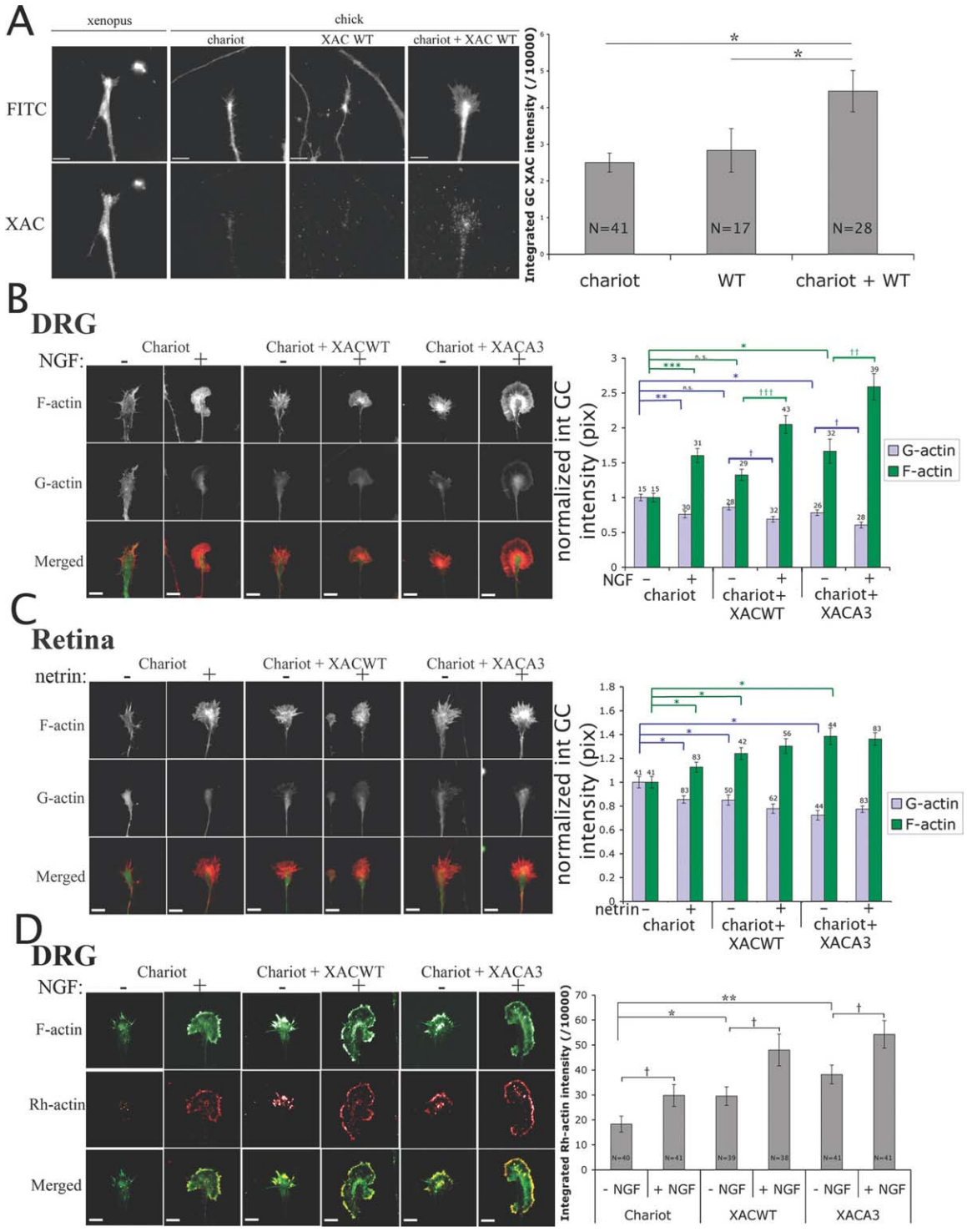

Figure 5

increase in proximal UtrCH intensity induced by the Chariot-XACA3 gradient was not due to a local increase in volume.

Taken together, these studies indicate that gradients of NGF, netrin and Chariot-XACA3 induce attractive growth cone turning and increased F-actin distribution in growth cone regions proximal to the pipette tips. In addition, F-actin is more concentrated in growth cone regions containing higher AC activity. This is consistent with our earlier findings [Fig. 4(C)] that staining for phospho-AC (inactive AC) is lower in growth cone regions contacting NGF-beads than in regions free of NGF-beads or in regions contacting BSA-beads, as well as the increased permeabilization-resistant ADF in growth cone regions proximal to a NGF or netrin gradient [Fig. 4(D)].

Our evidence suggests that NGF induces attractive DRG growth cone turning by locally activating AC, which stimulates local actin polymerization in the growth cone region proximal to NGF. In support of this, we showed that a gradient of cell-permeable AC induces growth cone turning with both increased AC content and increased F-actin in the growth cone side toward the AC source. To further examine the role of asymmetric AC activity in mediating growth cone turning, we introduced an NGF gradient to growth cones in the presence of globally applied Chariot-A3 to raise AC activity throughout the growth cone and diminish NGF-induced asymmetry in AC activity [Fig. 7(B)]. We found the average turning angle to NGF was reduced compared to NGF turning in the absence of Chariot-A3, although the difference was not statistically significant ($p = 0.099$). In like manner, the mean turning angle to a Chariot-A3 gradient was also reduced by global elevation of NGF, compared to A3 turning in the absence of NGF (but not statistically significant, $p = 0.23$). In both cases, NGF gradient with global Chariot-A3 and Chariot-A3 gradient with global NGF, the average turning angle was significantly greater than turning toward a Chariot-BSA gradient ($p < 0.05$). These data suggest that a small asymmetry in ADF/cofilin activity across a growth cone can elicit attractive turning, but the reduced turning angles observed with diminished AC asymmetry provides further support that turning toward positive cues is mediated by intracellular asymmetry of AC activity. Furthermore, activation of additional proteins downstream of NGF signaling, including paxillin (Khan et al., 1995), integrins (Grabham and Goldbert, 1997), and microtubule plus end binding protein APC (Zhou et al., 2004) also likely affect growth cone trajectories in addition to AC activation.

Reducing AC Activation or Protein Levels Blocks NGF- and Netrin-Induced Growth Cone Protrusion and Turning

If local AC activation is necessary for attractive turning toward NGF and netrin, we would expect that blocking AC activation will block attractive responses to these cues. To test this, we transfected neurons with either a constitutively active LIMK construct (CA-LIMK) to maintain high levels of phosphorylated inactive AC, with a plasmid expressing GFP and a hairpin RNA that generates a small interfering siRNA against chick ADF, or with a GFP- control RNAi plasmid. As expected, neurons transfected with CA-LIMK and cultured 24 h had higher levels of phospho-AC compared to GFP-transfected controls [Fig. S4(A)]. Neurons transfected with ADF-RNAi for 48 h showed reduced ADF immunostaining, compared to GFP- control RNAi transfected cells or nontransfected cells [Fig. S4(C)], and Western blot

Figure 5 Increased AC activity results in increased F-actin, decreased G-actin, and increased F-actin barbed ends. One microgram of XACWT or XACA3 in PBS was complexed with Chariot reagent in dH20 for 30 min. Panel A shows chick DRG explants treated 1 h with chariot, XACWT alone, or chariot + XACWT, and fixed and stained with the anti-*Xenopus* AC antibody XAC1. The leftmost pair of images show a growth cone of a *Xenopus* spinal neuron stained robustly with XAC1. The histogram shows integrated XAC1 growth cone intensities for chick DRGs shown. For panels B–D, Chariot alone or with recombinant proteins added to DRG (B and D) or temporal retina (C) explants 1 h before addition of control media, 40 ng/mL NGF (B and D) or 500 ng/mL netrin (C) for 15 min. Panels B and C show growth cones fixed and stained for F-actin (Alexa Fluor 568-phalloidin, red) and G-actin (fluorescein- DNase1, green), and mean integrated growth cone (int GC) fluorescence intensities are expressed normalized to Chariot, media controls. Panel D shows DRG growth cones that were permeabililzed with Alexa Fluor 488-phalloidin for 1 min (green), then incubated 4 min with 0.45 μM rhodamine-G actin (red) before being fixed and imaged. Mean growth cone fluorescence intensities of phalloidin staining and Rh-actin were determined. Statistical significance using ANOVA are indicated with "*," significance using Student's *t* test are indicated with "†." Data are Means ± SEM; $*p < 0.05$; $**p < 0.001$; $***p < 0.0001$. Scale bars: 10 μm.

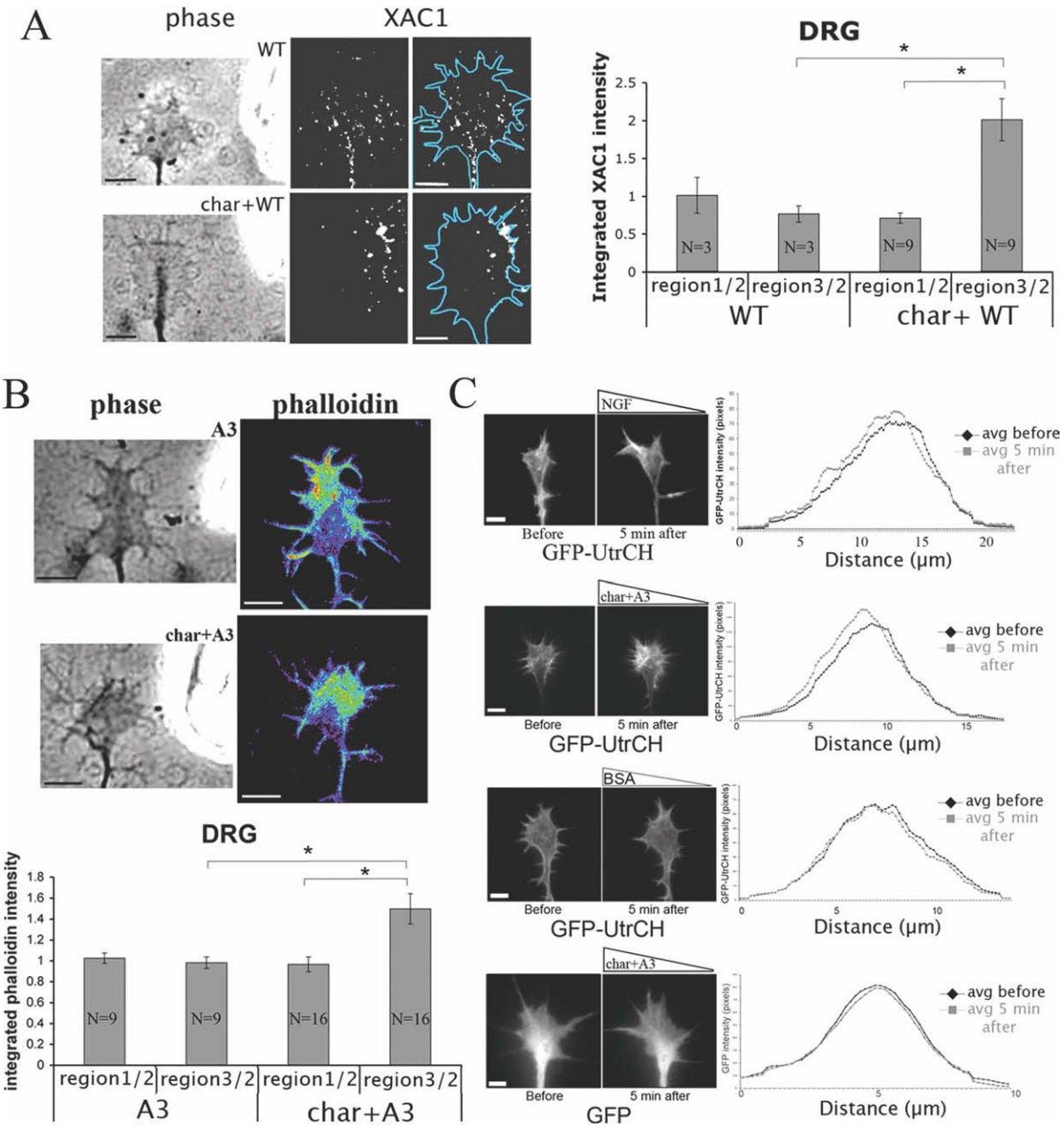

Figure 6 Growth cones exposed to a gradient of XACA3 exhibit asymmetrical F-actin distribution. For panel A, DRG growth cones were subjected to XACWT or chariot complexed with XACWT diffusing from a micropipette for 15 min, fixed and stained with XAC1, and quantified as in Figure 3(B). Data was taken from 3 separate days. Panel B shows F-actin (Alexa Fluor 488-phalloidin) distribution (pseudo-colored) in DRG growth cones subjected for 15 min to XACA3 or chariot + XACA3 diffusing from a micropipette, and quantified as in Figure 3(B). Panel C shows distribution of GFP-UtrCH or GFP in transfected DRG growth cones that were exposed at one side to a pipette tip releasing NGF (data as reported in Roche et al., 2009), chariot-A3 or chariot-BSA complexes. An image was taken before and 5 min after pipette introduction. The distribution of fluorescence is expressed as the intensity along a 15 pixel-wide line across the growth cone width. Statistical significance using ANOVA. Data are Means ± SEM; $*p < 0.05$. Scale bars: 10 μm.

analysis showed ADF protein level was reduced in ADF-RNAi transfected chick embryo fibroblasts [Fig. S4(B)].

We then examined growth cone responses to NGF in transfected DRG growth cones. As expected, in GFP-control RNAi DRG growth cones, leading edge

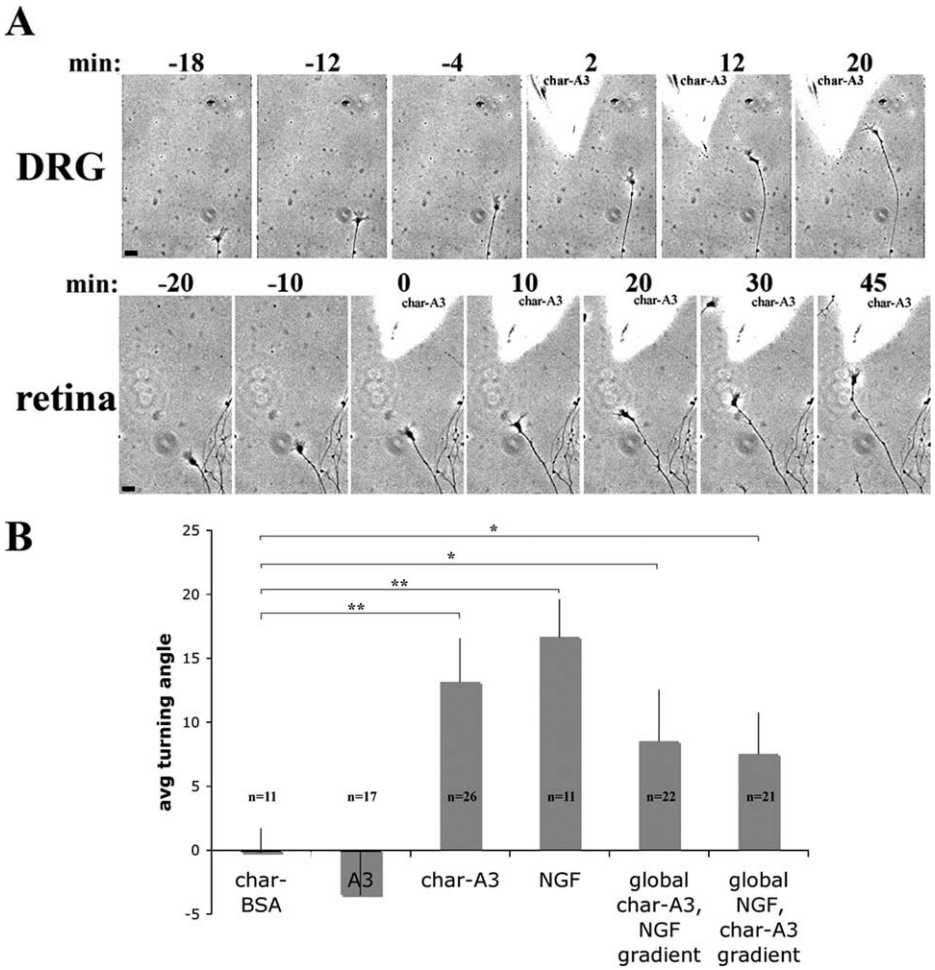

Figure 7 Growth cones exposed to a gradient of cell-permeable AC exhibit attractive turning. Panel A shows time-lapse images of a DRG and a retinal growth cone turning toward a gradient of chariot-A3 diffusing from the micropipette. Time shows minutes relative to addition of the micropipette. Panel B shows average turning angles of DRG growth cones to various gradients. Statistical significance using Student's *t* test. Data are Means ± SEM; $*p < 0.05$; $**p < 0.001$. Scale bars: 20 μm.

protrusion increased immediately after adding NGF. Remarkably, growth cones expressing CA-LIMK or ADF RNAi had no protrusion increase following NGF addition [Fig. 8(A)]. Furthermore, compared to GFP controls, CA-LIMK expressing DRG neurons showed reduced attractive turning to NGF [Fig. 8(B)], and the turning of retinal growth cones toward a netrin-coated micropipette was also reduced in CA-LIMK expressing retinal neurons [Fig. 8(C)]. Bath application of K252a, an inhibitor of the NGF receptor TrkA, also abolished turning toward NGF. Although the growth cones of CA-LIMK transfected DRG neurons advanced slower than GFP controls (1.4 ± 0.04 μm/min for GFP, 1.18 ± 0.16 μm/min for CA-LIMK), growth cones were observed 60 min, long enough to advance more than 60 μm and complete a turning response. These data suggest that AC activation by NGF or netrin is necessary for membrane protrusion and attractive turning to NGF or netrin.

Restoring Active AC to CA-LIMK and ADF RNAi Growth Cones Rescues Membrane Protrusion

To determine if the block of NGF-induced membrane protrusion was specifically caused by the reduced AC activity, we added Chariot + XACA3 protein to GFP-control RNAi, CA-LIMK, or ADF RNAi-expressing growth cones, and examined leading edge dynamics. As seen in Figure 9, the addition of Chariot-XACA3 proteins increased growth cone protrusion in DRG neurons transfected with either of the three plasmids. These data support the notion that the reduction in

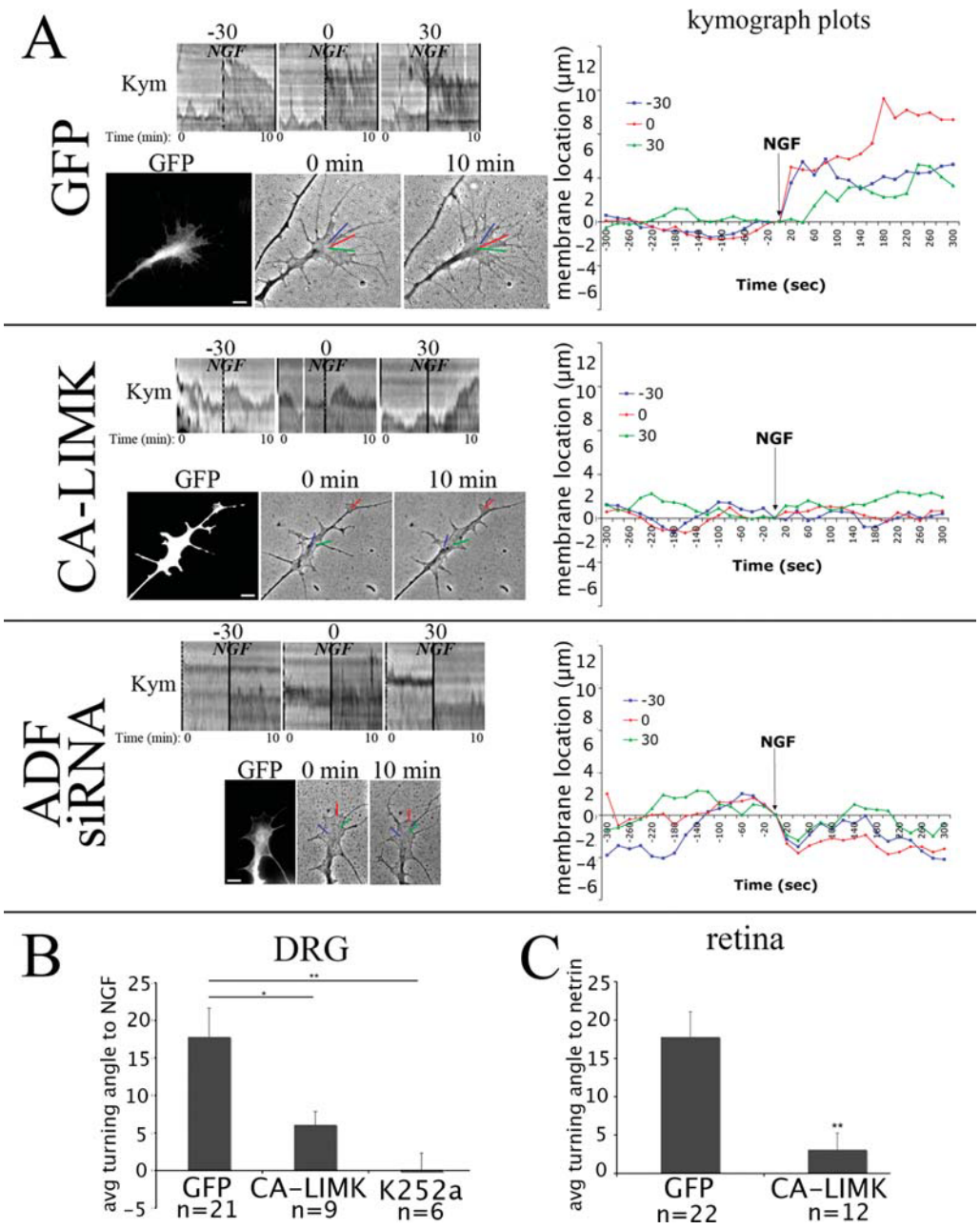

Figure 8 Reducing AC activation or protein levels blocks NGF- and netrin-induced membrane protrusion and guidance. Panel A shows DRGs that were transfected with GFP-RNAi control, GFP + CA-LIMK, or ADF-RNAi and cultured 48 h on L1. Transfected growth cones were imaged at 10 s intervals for 5 min before and after the addition of 40 ng/mL NGF, and kymographs of the leading edge were generated. Quantification of membrane dynamics were performed as in Figure 1 ($n = 5$). DRG (B) or retinal neurons (C) were transfected with GFP or GFP + CA-LIMK, cultured 48 h, and subjected to a gradient of NGF (B) or netrin-1 (C), and mean turning angles were measured. In B, nontransfected DRG growth cones were treated with 500 n*M* Trk inhibitor K252a 3 min prior to NGF-pipette introduction. Statistical significance using Student's *t* test. Data are Means ± SEM; $*p < 0.05$; $**p < 0.001$. Scale bars: 10 μm. [Color figure can be viewed in the online issue, which is available at www.interscience.wiley.com.]

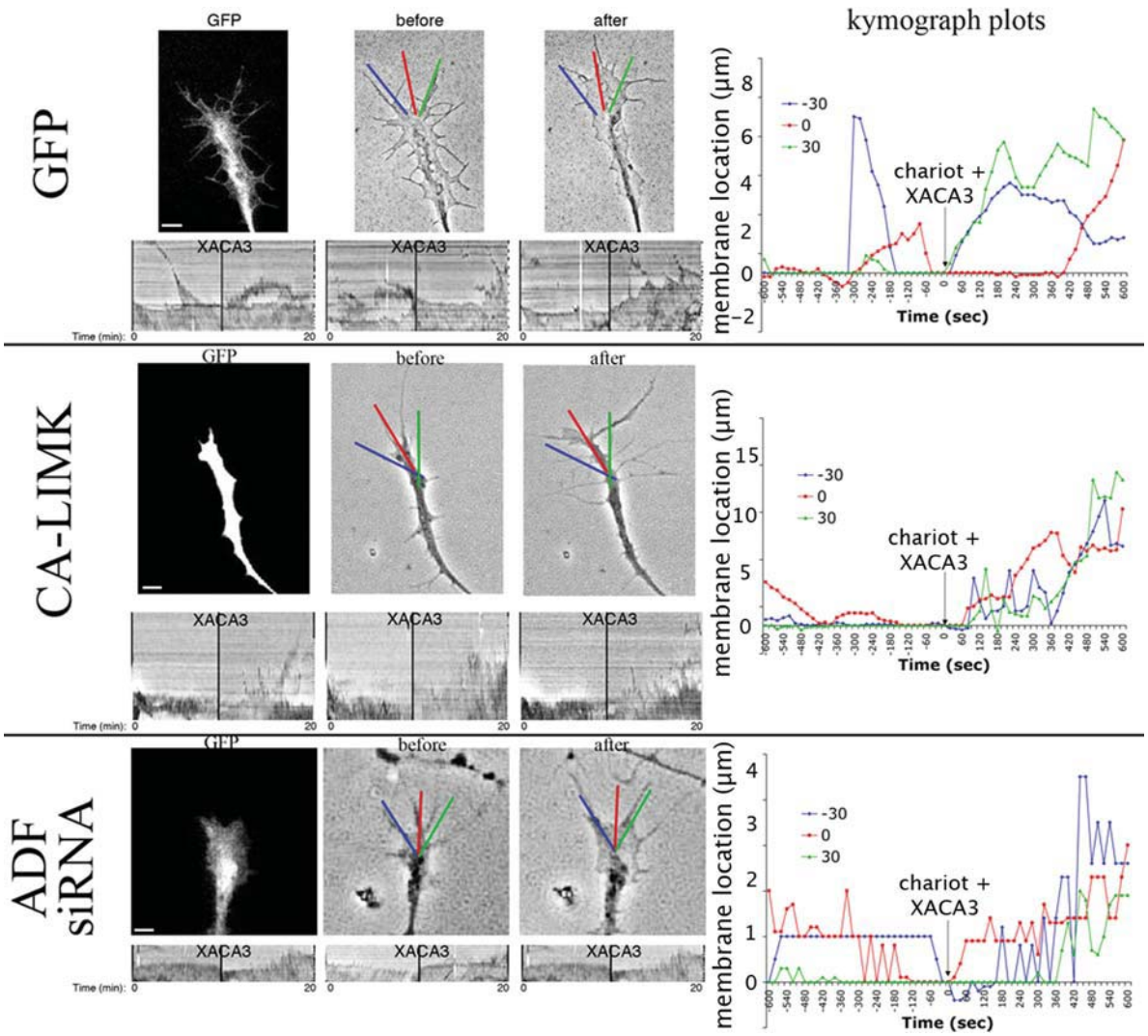

Figure 9 Restoring active AC to CA-LIMK- and ADF-RNAi-expressing growth cones rescues membrane protrusion. DRG neurons were transfected with GFP-RNAi control, GFP + CA-LIMK, or ADF-RNAi, and cultured for 48 h on L1. Transfected growth cones were imaged every 10 s for 10 min before and after the addition of chariot complexed with XACA3. Quantification of membrane dynamics were performed as in Figure 1. Scale bars: 10 μm. [Color figure can be viewed in the online issue, which is available at www.interscience.wiley.com.]

NGF-induced protrusion seen in CA-LIMK and ADF RNAi-expressing growth cones is due to reduced AC levels and not to other factors associated with the constructs.

Actin Protein Levels are Higher in Chick DRG Growth Cones Compared to Xenopus Laevis Spinal Neuronal Growth Cones

Our data suggest a local increase in AC activity can induce growth cone turning toward the side with higher activity. This finding is in direct contrast with that of Wen et al. (2007), where *Xenopus* spinal neuronal growth cones responding to bone morphogenic protein 7 (BMP7) turned toward the side with lower AC activity and away from the side with higher AC activity. Recent studies have found differing effects on actin organization at different ratios of AC to actin (Blanchoin and Pollard, 1999; Chen et al., 2004; Andrianantoandro and Pollard, 2006; Pavlov et al., 2007; Chan et al., 2009). We, therefore, sought to compare actin protein levels in chick and *Xenopus* spinal neuronal growth cones. Using immunocytochemistry, we stained chick DRG and *Xenopus* spinal neuron cultures simultaneously, using multiple antibodies

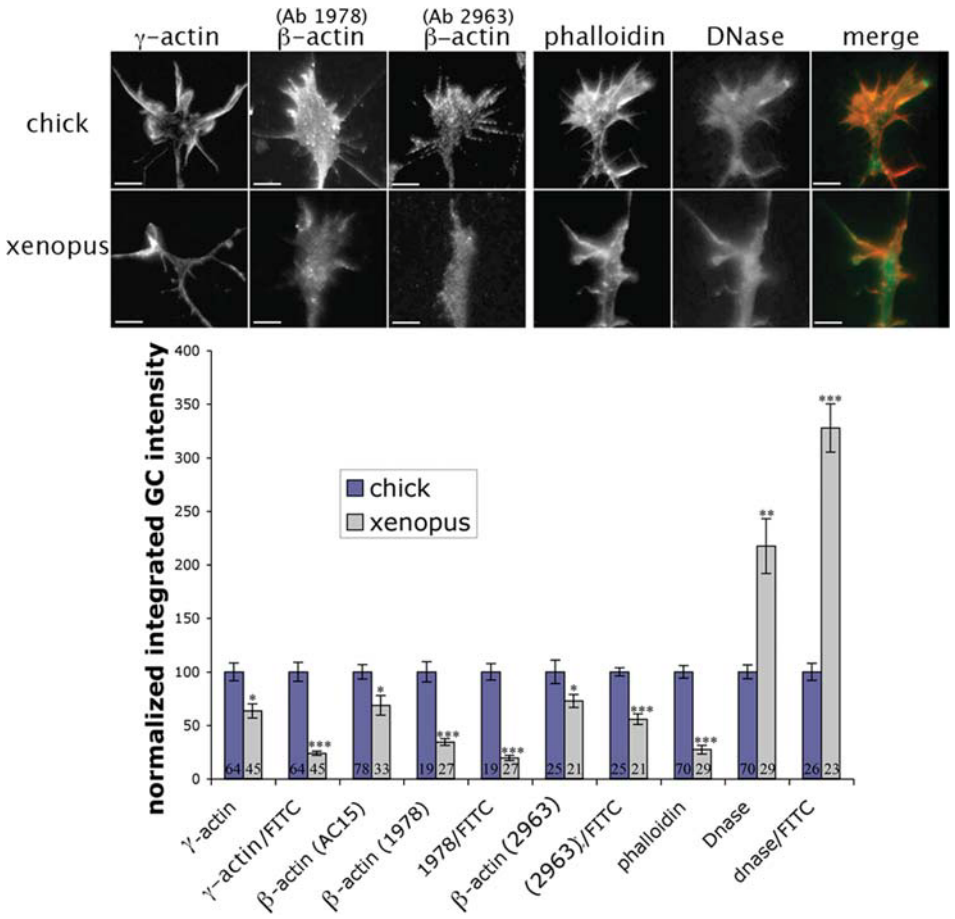

Figure 10 Chick DRG growth cones contain higher levels of actin compared to Xenopus spinal neuronal growth cones. Cultured chick DRG and Xenopus spinal neurons were labeled with antibodies against γ-actin (ab 7577), β-actin (AC15, Abcam; A1978 Sigma), actin (2963, James Ervasti), Alexa-Fluor 488 DNase (green), or Alexa-fluor 568 phalloidin (red). Where primary antibodies were not conjugated to FITC (γ-actin, A1978, 2963), FITC was used as a control for total protein. Integrated growth cone intensities were measured and normalized to chick. Statistical significance using Student's t test. Data are Means $\pm$ SEM; *$p < 0.05$; **$p < 0.001$; ***$p < 0.0001$. Scale bars: 10 μm. [Color figure can be viewed in the online issue, which is available at www.interscience.wiley.com.]

against β- and γ-actin. The very high sequence conservation for β- and γ-actin among vertebrates suggests that these antibodies should recognize these actin isoforms similarly in frog and chick neurons. The integrated (sum) intensity was measured and normalized to total protein (FITC), except with FITC-conjugated AC15. Measurements of integrated growth cone intensities indicated lower levels of both γ-actin and β-actin in *Xenopus* growth cones compared to chick (see Fig. 10). These differences remained consistent with multiple antibodies, and when measured as a ratio to total protein using FITC (see Fig. 10). In addition, we found *Xenopus* growth cones had higher levels of DNase and lower levels of phalloidin staining, suggesting *Xenopus* growth cones have a higher G-actin:F-actin ratio compared to chick DRG growth cones.

We do not know the relative concentrations or basal activity of AC in chick versus *Xenopus*, nor possible differences in additional actin-binding proteins. Although further research is needed to determine if these actin differences are sufficient to account for these disparate results, it is not unreasonable to suggest that basal differences in actin expression could affect the net response of growth cones responding to guidance cues. For example, recent studies have shown local protein synthesis is important in growth cone guidance (Campbell and Holt, 2001; Piper and Holt, 2004; Wu et al., 2005), and specifically, local translation of β-actin mRNA in *Xenopus* growth cones (Leung et al., 2006; Yao et al., 2006). However, we recently reported normal growth cone guidance with chick and mouse neurons in the presence of

protein synthesis inhibitors (Roche et al., 2009). These data suggest that in growth cones containing less actin, guidance cue-induced local protein synthesis may be more essential for growth cone turning compared to growth cones with higher actin levels, where reorganization of existing actin is sufficient. In the present study, these relative differences in actin levels and organization could affect how activated AC modifies actin filament dynamics.

DISCUSSION

Here, we have shown that two attractive cues, NGF and netrin, increase leading edge protrusion in DRG and retinal growth cones, respectively, through increases in F-actin and actin polymerization. These guidance cues decrease inactive (phosphorylated) AC levels in growth cones. Direct elevation of AC activity in DRGs also increases free actin barbed ends and F-actin levels. A diffusible gradient of NGF, netrin, or cell-permeable AC stimulates proximal F-actin assembly in growth cones, and elicits attractive turning. Reducing AC activity or protein level blocks guidance cue-induced membrane protrusion and blunts guidance cue-induced attractive turning for DRG and retinal growth cones. These data support a model in which NGF and netrin stimulate attractive turning through local activation of AC, which promotes actin polymerization in the growth cone side toward the guidance cue.

The regulation of actin organization and dynamics by guidance cue signaling has been a focus of growth cone research (Pak et al., 2008; Lowery and Van Vactor, 2009). Applied globally, repulsive cues reduce growth cone F-actin and protrusion, while attractive cues promote protrusion and increased F-actin (Fan et al., 1993; Gallo and Letourneau, 2000; Zhou and Cohen, 2003; Kalil and Dent, 2005; Brown and Bridgman, 2009; Roche et al., 2009). Specifically, global application of NGF and netrin-1 have been linked to increases in F-actin (Seeley and Greene, 1983; Goldberg et al., 2000; Shekarabi and Kennedy, 2002; Lebrand et al., 2004). More akin to guidance situations, local application of NGF and netrin, were shown to locally promote protrusive activity and increased F-actin (Gallo et al., 1997; Gallo and Letourneau, 1998, 2000; Dent et al., 2004; Chang et al., 2006), and recent studies have shown gradients of netrin-1 and brain-drived neurotrophic factor induce proximal increases in β-actin synthesis in *Xenopus* growth cones (Leung et al., 2006; Yao et al., 2006). However, in the nearly 2 decades of work linking F-actin increases to attractive cues, we understand relatively little about the mechanisms underlying these changes. And despite the identification of numerous actin-binding proteins with diverse effects on actin organization, links between specific proteins downstream of specific guidance cues are not well characterized (Suter and Forscher, 1998; Dent and Gertler, 2003; Huber et al., 2003; Pak et al., 2008; Lowery and Van Vactor, 2009).

In this article, we looked more closely at the role of actin polymerization in growth cone responses to attractive guidance cues. We quantified the increased F-actin in growth cones exposed to globally applied NGF and netrin and the distribution of increased F-actin in growth cones exposed to gradients of these cues. To probe the specific changes in actin organization responsible for these increases, we measured, for the first time, the effects of guidance cues on F-actin barbed ends, which are the sites of actin polymerization. We found that barbed ends are increased throughout growth cones by global NGF exposure and locally in growth cone margins that are proximal to gradients of NGF (DRG) or netrin (retina). We also measured retrograde actin flow, which if reduced, could contribute to increased F-actin in the growth cone leading margin. We found that NGF exposure did not change the retrograde actin flow rate, suggesting increased actin polymerization is the primary mechanism for the increased F-actin induced in the growth cone leading margin by attractive cues. In migratory cells, similar local stimulation of leading edge actin polymerization is critical for cell polarity and directed migration to chemoattractants (Weiner et al., 1999; Pollard and Borisy, 2003; Charest and Firtel, 2007).

Our results indicate that local activation of the actin regulatory protein ADF/cofilin (AC) is a necessary component of attractive growth cone guidance. Previous work showed that NGF and the related neurotrophin BDNF activate AC in conjunction with neurotrophin-induced increases in motility and filopodial dynamics (Meberg et al., 1998; Gehler et al., 2004; Chen et al., 2006). Similarly, we found that global addition of NGF or netrin reduced total growth cone levels of inactive phospho-AC, and regions of DRG growth cones contacting NGF-coupled beads also had reduced phospho-AC. When growth cones were exposed to NGF (DRG) or netrin (retina) gradients and permeabilized before fixation to release inactive phospho-AC, subsequent immunostaining for remaining ADF bound to the actin cytoskeleton was concentrated in the growth cone region toward the attractive cue, further indicating that AC activity was higher proximal to an attractant. When we reduced AC activity by RNAi or by expressing con-

stitutively active LIMK to inactivate AC by phosphorylation, growth cones failed to respond to attractive guidance cues, indicating the necessity of AC activity for attractive turning to NGF or netrin.

Similar to the effects of NGF and netrin exposure, we found the content of F-actin barbed ends in DRG and retinal growth cones was increased by incorporation of cell-permeable AC, and when DRG or retinal growth cones were subjected to a gradient of cell-permeable AC, the asymmetric incorporation of AC resulted in both increased F-actin and attractive growth cone turning toward the source of cell-permeable AC. This demonstrates the sufficiency of elevated AC activity for barbed end creation, actin polymerization, and attractive growth cone turning, and is similar to the role of AC in promoting actin polymerization at the front of chemotaxing carcinoma cells (Zebda et al., 2000; Ghosh et al., 2004; Mouneimne et al., 2004, 2006).

Biochemical studies have revealed the complexity of AC in regulating actin filament turnover (for review, see Carlier et al., 1997; Van Troys et al., 2008). Some studies suggest AC activity enhances monomer loss from F-actin pointed ends, thereby replenishing the actin monomer pool (Carlier et al., 1997; Maciver et al., 1998; Cramer, 1999), whereas other studies attribute increased actin polymerization to AC-mediated severing of F-actin that increases barbed ends for monomer addition (McGough et al., 1997; Du and Frieden, 1998). The ratio of AC:actin is another factor in actin dynamics. At low AC levels relative to actin, cofilin binds actin independently, promoting filament turnover and polymerization at new barbed ends. (Andrianantoandro and Pollard, 2006). At intermediate concentrations, cofilin binds actin cooperatively and rapidly severs actin filaments (Blanchoin and Pollard, 1999; Andrianantoandro and Pollard, 2006; Pavlov et al., 2007; Chan et al., 2009). At high relative concentration, cofilin can both nucleate and rapidly sever actin but then stabilizes filaments as they become saturated with cofilin (Chen et al., 2004; Andrianantoandro and Pollard, 2006; Pavlov et al., 2007). Beyond these studies with purified components, the net roles of AC become more complex and varied within cells, where multiple factors, including the G-actin pool size, components that regulate AC activity, and the actions of additional actin regulatory proteins are integrated in determining actin filament organization and dynamics in migrating cells (Ressad et al., 1999; Sarmiere and Bamburg, 2003; Bernstein and Bamburg, 2010).

Such complexity in regulating actin filaments may indicate why our result concerning AC activity and growth cone turning differs from that of Wen et al. (2007), where *Xenopus* growth cones responded to BMPs by turning toward the side with lower AC activity. We probed other differences between *Xenopus* and chick growth cones and found *Xenopus* growth cones have lower levels of actin and lower F-actin/G-actin ratios compared to chick growth cones, which may impact how actin is re-organized when AC activity increases. An additional consideration is that BMP-receptor signaling may involve different pathways and activities than what is activated downstream of netrin-1 and NGF. For example, netrin-mediated actin polymerization requires the anti-capping activity of Ena/VASP (Gitai et al., 2003; Gomez and Robles, 2004; Lebrand et al., 2004). The GTPase Rac, which is activated by both NGF and netrin (Ridley et al., 1992; Gitai et al., 2003), activates SCAR to enhance the actin nucleating activity of the Arp2/3 complex (Machesky et al., 1999). The actin nucleating and F-actin branching actions of the Arp2/3 complex may interact with the filament severing and debranching actions of AC in a variety of ways to regulate actin organization during lamellipodial and filopodial protrusion (Ressad et al., 1999; Svitkina and Borisy, 1999; Blanchoin et al., 2000; Ichetovkin et al., 2002; Chan et al., 2009). Further, the relative activities of F-actin capping and actin-sequestering proteins directly control the fundamental elements of actin polymerization, free barbed ends and G-actin monomer. Thus, the integration of all actin regulatory activities may dictate that different levels of AC activity should exist in different growth cones to mediate attractive growth cone turning. In *Xenopus* growth cones increased filopodial protrusion and F-actin accumulation may require low AC activity, whereas in chick growth cones, increased AC activity promotes actin polymerization to drive protrusion and attractive turning to NGF and netrin.

This article does not address the mechanisms by which NGF and netrin regulate AC activity, which is becoming a more complex topic (Bernstein and Bamburg, 2010). NGF- and netrin-induced dephosphorylation of AC could occur through activation of a phosphatase or a decrease in kinase activity. Several phosphatases activate AC, including chronophin (Gohla et al., 2005), and isoforms of slingshot, which was recently implicated in carcinoma cell chemotaxis (Niwa et al., 2002; Eiseler et al., 2009). Inactivation of AC is mediated by LIM and TES kinases (Yang et al., 1998; Toshima et al., 2001). LIMK is active when phosphorylated by PAK1, PAK4, or Rho-kinase (ROCK), and is inhibited by dephosphorylation by SSH phosphatase or ubiquitination by Rnf6 (for review, see Bernard, 2007). In addition, several feedback loops may play important roles, such as SSH

activation by F-actin, or LIMK inactivation by SHH. Additional regulators of AC include 14-3-3 proteins, which promote inactive phospho-AC by directly binding to phospho-AC and LIMK (Gohla and Bokoch, 2002), and incorporation of 14-3-3 into retinal growth cones blocks BDNF-mediated activation of AC (Gehler et al., 2004). AC activity is also regulated by pH, phosphoinositides, and other proteins such as tropomyosin or Aip1 (for review, see Sarmiere and Bamburg, 2003). In summary, multiple regulators affect AC activity.

In summary, our data support a model in which two important cues, NGF and netrin, induce attractive growth cone turning by locally activating AC and stimulating actin polymerization in growth cone regions proximal to the guidance cue source. Further studies are needed to clarify how the activities of multiple actin-binding proteins and associated regulatory factors are integrated to mediate the effects of guidance cues on growth cone trajectories.

The authors thank Florence Roche for technical assistance, Alisa Shaw for assistance in recombinant XACA3 protein purification, and Dr. O'Neil Wiggan for preparing the cell extracts and running the western blot on the hairpin RNA for silencing ADF.

REFERENCES

Andrianantoandro E, Pollard TD. 2006. Mechanism of actin filament turnover by severing and nucleation at different concentrations of ADF/cofilin. Mol Cell 24:13–23.

Arber S, Barbayannis FA, Hanser H, Schneider C, Stanyon CA, Bernard O, Caroni P. 1998. Regulation of actin dynamics through phosphorylation of cofilin by LIM-kinase. Nature 393:805–809.

Bamburg JR, Bray D. 1987. Distribution and cellular localization of actin depolymerizing factor. J Cell Biol 105:2817–2825.

Barak LS, Nothnagel EA, DeMarco EF, Webb WW. 1981. Differential staining of actin in metaphase spindles with 7-nitrobenz-2-oxa-1, 3-diazole-phallacidin and fluorescent DNase: Is actin involved in chromosomal movement? PNAS 78:3034–3038.

Bentley D, O'Connor TP. 1994. Cytoskeletal events in growth cone steering. Curr Opin Neurobiol 4:43–48.

Bentley D, Toroian-Raymond A. 1986. Disoriented pathfinding by pioneer neurone growth cones deprived of filopodia by cytochalasin treatment. Nature 323:712–715.

Bernard O. 2007. Lim kinases, regulators of actin dynamics. Int J Biochem Cell Biol 39:1071–1076.

Bernstein BW, Bamburg JR. 2010. ADF/cofilin: A functional node in cell biology. Trends Cell Biol 20:187–195.

Birkenfeld J, Betz H, Roth D. 2001. Inhibition of neurite extension by overexpression of individual domains of LIM kinase 1. J Neurochem 78:924–927.

Blanchoin L, Pollard TD. 1999. Mechanisms of interaction of Acanthoemba actophorin (ADF/cofilin) with actin filaments. J Biol Chem 274:15538–15546.

Blanchoin L, Pollard TD, Mullins RD. 2000. Interactions of ADF/cofilin. Arp2/3 complex, capping protein and profilin in remodeling of branched actin filament networks. Curr Biol 10:1273–1282.

Brown JA, Bridgman PC. 2009. Disruption of the cytoskeleton during Semaphorin 3A induced growth cone collapse correlates with differences in actin organization and associated binding proteins. Dev Neurobiol 69:633–646.

Brummelkamp TR, Bernards R, Agami R. 2002. A system for stable expression of short interfering RNAs in mammalian cells. Science 296:550–553.

Burkel BM, von Dassow G, Bement WM. 2007. Versatile fluorescent probes for actin filaments based on the actin-binding domain of utrophin. Cell Motil Cytoskeleton 64:822–832.

Campbell DS, Holt CE. 2001. Chemotropic responses of retinal growth cones mediated by rapid local protein synthesis and degradation. Neuron 32:1013–1026.

Carlier MP, Laurent V, Santolini J, Melki R, Didry D, Xia GX, Hong Y, et al. 1997. Actin depolymerizing factor (ADF/cofilin) enhances the rate of filament turnover: Implication in actin-based motility. J Cell Biol 136: 1307–1322.

Casaccia-Bonnefil P, Gu C, Chao MV. 1999. Neurotrophins in cell survival/death decisions. Adv Exp Med Biol 468:275–282.

Chan AY, Raft S, Bailly M, Wyckoff JB, Segall JE, Condeelis JS. 1998. EGF stimulates an increase in actin nucleation and filament number at the leading edge of the lamellipod in mammary adenocarcinoma cells. J Cell Sci 111:199–211.

Chan C, Beltzner CC, Pollard TD. 2009. Cofilin dissociates Arp2/3 complex and branches from actin filaments. Curr Biol 19:1–9.

Chan CE, Odde DJ. 2008. Traction dynamics of filopodia on compliant substrates. Science 322:1687–1691.

Charest PG, Firtel RA. 2007. Big roles for small GTPases in the control of directed cell movement. Biochem J 401:377–390.

Chen H, Bernstein BW, Sneider JM, Boyle JA, Minamide LS, Bamburg JR. 2004. In vitro activity differences between proteins of the ADF/cofilin family define two distinct subgroups. Biochemistry 43:7127–7142.

Chen TJ, Gehler S, Shaw AE, Bamburg JR, Letourneau PC. 2006. Cdc42 participates in the regulation of ADF/cofilin and retinal growth cone filopodia by brain derived neurotrophic factor. J Neurobiol 66:103–114.

Chen WP, Chang YC, Hsieh ST. 1999. Trophic interactions between sensory nerves and their targets. J Biomed Sci 6:79–85.

Cramer LP. 1999. Role of actin-filament disassembly in lamellipodium protrusion in motile cells revealed using the drug jasplakinolide. Curr Biol 9:1095–1105.

Davies AM. 2000. Neurotrophins: More to NGF than just survival. Curr Biol 10:R374–R376.

Dent EW, Barnes AM, Tang F, Kalil K. 2004. Netrin-1 and semaphorin 3A promote or inhibit cortical axon branching, respectively, by reorganization of the cytoskeleton. J Neurosci 24:3002–3012.

Dent EW, Gertler FB. 2003. Cytoskeletal dynamics and transport in growth cone motility and axon guidance. Neuron 40:209–227.

Devineni N, Minamide LS, Niu M, Safer D, Verma R, Bamburg JR, Nachmias VT. 1999. A quantitative analysis of G-actin binding proteins and the G-actin pool in developing chick brain. Brain Res 823:129–140.

Du J, Frieden C. 1998. Kinetic studies on the effect of yeast cofilin on yeast actin polymerization. Biochem 37:13276–13284.

Eiseler T, Doeppler H, Yan IK, Kitatani K, Mizuno K, Storz P. 2009. Protein kinase D1 regulates cofilin-mediated F-actin reorganization and cell motility through slingshot. Nat Cell Biol 11:545–556.

Endo M, Ohashi K, Sasaki Y, Goshima Y, Niwa R, Uemura T, Mizuno K. 2003. Control of growth cone motility and morphology by LIM kinase and Slingshot via phosphorylation and dephosphorylation of cofilin. J Neurosci 23:2527–2537.

Fan J, Mansfield SG, Redmond T, Gordon-Weeks PR, Raper JA. 1993. The organization of F-actin and microtubules in growth cones exposed to a brain-derived collapsing factor. J Cell Biol 121:867–878.

Frantz C, Barreiro G, Dominguez L, Chen X, Eddy R, Condeelis J, Kelly MJ, et al. 2008. Cofilin is a pH senor for actin free barbed end formation: role of phosphoinositite binding. J Cell Biol 183:865–879.

Gallo G, Lefcort FB, Letourneau PC. 1997. The trkA receptor mediates growth cone turning toward a localized source of nerve growth factor. J Neurosci 17:5445–5454.

Gallo G, Letourneau PC. 1998. Localized sources of neurotrophins initiate axon collateral sprouting. J Neurosci 18:5403–5414.

Gallo G, Letourneau PC. 2000. Neurotrophins and the dynamic regulation of the neuronal cytoskeleton. J Neurobiol 44:159–173.

Gallo G, Letourneau PC. 2004. Regulation of growth cone actin filaments by guidance cues. J Neurobiol 58:92–102.

Garvalov BK, Flynn KC, Neukirchen D, Meyn L, Teusch N, Wu X, Brakebusch C, et al. 2007. Cdc42 regulates cofilin during the establishment of neuronal polarity. J Neurosci 27:13117–13129.

Gehler S, Shaw AE, Sarmiere PD, Bamburg JR, Letourneau PC. 2004. Brain-derived neurotrophic factor regulation of retinal growth cone filopodial dynamics is mediated through actin depolymerizing factor/cofilin. J Neurosci 24:10741–10749.

Ghosh M, Song X, Mouneimne G, Sidani M, Lawrence DS, Condeelis JS. 2004. Cofilin promotes actin polymerization and defines the direction of cell motility. Science 304:743–746.

Gitai Z, Yu TW, Lundquist EA, Tessier-Lavigne M, Bargmann CI. 2003. The netrin receptor UNC-40/DCC stimulates axon attraction and outgrowth through enabled and, in parallel. Rac and UNC-115/Ab LIM. Neuron 37:53–65.

Glebova NO, Ginty DD. 2004. Heterogeneous requirement of NGF for sympathetic target innervation *in vivo*. J Neurosci 24:743–751.

Gohla A, Birkenfeld J, Bokoch GM. 2005. Chronophin, a nover HAD-type serine protein phosphatase, regulates cofilin-dependent actin dynamics. Nat Cell Biol 7:21–29.

Gohla A, Bokoch GM. 2002. 14–3-3 Regulates actin dynamics by stabilizing phosphorylated cofilin. Curr Biol 12:1704–1710.

Goldberg DJ, Foley MS, Tang D, Grabham PW. 2000. Recruitment of the Arp2/3 complex and mena for the stimulation of actin polymerization in growth cones by nerve growth factor. J Neurosci Res 60:458–467.

Gomez TM, Harrigan D, Henley J, Robles E. 2003. Working with Xenopus spinal neurons in live cell culture. Methods Cell Biol 71:129–156.

Gomez TM, Robles E. 2004. The great escape: Phosphorylation of Ena/VASP by PKA promotes filopodial formation. Neuron 42:1–3.

Grabham PW, Goldberg DJ. 1997. Nerve growth factor stimulates the accumulation of ß1 integrin at the tips of filopodia in the growth cones of sympathetic neurons. J Neurosci 17:5455–5465.

Gunderson RW. 1985. Sensory neurite growth cone guidance by substrate absorbed nerve growth factor. J Neurosci Res 13:199–212.

Gunderson RW, Barrett JN. 1979. Neuronal chemotaxis: Chick dorsal-root axons turn toward high concentrations of nerve growth factor. Science 206:1079–1080.

Hanft LM, Rybakava IN, Patel JR, Rafael-Fortney JA, Ervasti JM. 2006. Cytoplasmic γ-actin contributes to a compensatory remodeling response in dystrophin-deficient muscle. PNAS 103:5385–5390.

Hassankhani A, Steinhelper ME, Soonpaa MH, Katz EB, Taylor DA, Andrade-Rozental A, Factor SM, et al. 1995. Overexpression of NGF within the heart of transgenic mice causes hyperinnervation, cardiac enlargement, and hyperplasia of ectopic cells. Dev Biol 169:309–321.

Henderson CE. 1996. Role of neurotrophic factors in neuronal development. Curr Opin Neurobiol 6:64–70.

Hotulainen P, Paunola E, Vartiainen MK, Lappalainen P. 2005. Actin-depolymerizing factor and cofilin-1 play overlapping roles in promoting rapid F-actin depolymerization in mammalian nonmuscle cells. Mol Biol Cell 16:649–664.

Huang TY, Minamide LS, Bamburg JR, Bokoch GM. 2008. Chronophin mediates an ATP-sensing mechanism for cofilin dephosphorylation and neuronal cofilin-actin rod formation. Dev Cell 15:691–703.

Huber AB, Kolodkin AL, Ginty DD, Cloutier JF. 2003. Signaling at the growth cone: Ligand-receptor complexes and the control of axon growth and guidance. Annu Rev Neurosci 26:509–563.

Ichetovkin I, Grant W, Condeelis J. 2002. Cofilin produces newly polymerized actin filaments that are preferred for dendritic nucleation by the Arp2/3 complex. Curr Biol 12:79–84.

Kalil K, Dent EW. 2005. Touch and go: Guidance cues signal to the growth cone cytoskeleton. Curr Opin Neurobiol 15:521–526.

Kennedy TE, Serafini T, de la Torre JR, Tessier-Lavigne M. 1994. Netrins are diffusible chemotropic factors for commissural axons in the embryonic spinal cord. Cell 78:425–435.

Khan MA, Okumura N, Okada M, Kobayashi S, Nakagawa H. 1995. Nerve growth factor stimulates tyrosine phosphorylation of paxillin in PC12h cells. FEBS Lett 362:201–204.

Korobova F, Svitkina T. 2008. Arp2/3 complex is important for filopodia formation, growth cone motility, and neuritogenesis in neuronal cells. Mol Biol Cell 19:1561–1574.

Kozma R, Sarner S, Ahmed S, Lim L. 1997. Rho family GTPases and neuronal growth cone remodeling relationship between increased complexity induced by Cdc42Hs, Rac, and Acetycholine and collapse induced by RhoA and Lysophosphatidic acid. Mol Cell Biol 17:1201–1211.

Kuhn TB, Meberg PJ, Brown MD, Bernstein BW, Minamide LS, Jensen JR, Okada K, et al. 2000. Regulating actin dynamics in neuronal growth cones by ADF/cofilin and rho family GTPases. J Neurobiol 44:126–144.

Lebrand C, Dent EW, Strasser GA, Lanier LM, Krause M, Svitkina TM, Borisy GG, et al. 2004. Critical role of Ena/VASP proteins for filopodia formation in neurons and in function downstream of netrin-1. Neuron 42:37–49.

Letourneau PC. 1978. Chemotactic response of nerve fiber elongation to nerve growth factor. Dev Biol 66:183–196.

Letourneau PC, Cypher C. 1991. Regulation of growth cone motility. Cell Motil Cytoskeleton 20:267–271.

Leung KM, van Horck FP, Lin AC, Allison R, Standart N, Holt CE. 2006. Asymmetrical beta-actin mRNA translation in growth cones mediates attractive turning to netrin-1. Nat Neurosci 9:1247–1256.

Lin CH, Forscher P. 1993. Cytoskeletal remodeling during growth cone-target interactions. J Cell Biol 121:1369–1383.

Lin CH, Thompson CA, Forscher P. 1994. Cytoskeletal reorganization underlying growth cone motility. Curr Opin Neurobiol 4:640–647.

Lowery LA, Van Vactor D. 2009. The trip of the tip: Understanding the growth cone machinery. Nat Rev Mol Cell Biol 10:332–343.

Machesky LM, Mullins RD, Higgs HN, Kaiser DA, Blanchoin L, May RC, Hall ME, et al. 1999. Scar, a WASp-related protein, activates nucleation of actin filaments by the Arp2/3 complex. Proc Natl Acad Sci USA 96:3739–3744.

Maciver SK, Pope BJ, Whytock S, Weeds AG. 1998. The effect of two actin depolymerizing factors (ADF/cofilins) on actin filament turnover: pH sensitivity of F-actin binding by human ADF, but not of Acanthamoeba actophorin. Eur J Biochem 256:388–397.

McGough A, Pope B, Chiu W, Weeds A. 1997. Cofilin changes the twist of F-actin: Implications for actin filament dynamics and cellular function. J Cell Biol 138:771–781.

Meberg PJ, Bamburg JR. 2000. Increase in neurite outgrowth mediated by overexpression of actin depolymerizing factor. J Neurosci 20:2459–2469.

Meberg PJ, Ono S, Minamide LS, Takahashi M, Bamburg JR. 1998. Actin depolymerizing factor and cofilin phosphorylation dynamics: Response to signals that regulate neurite extension. Cell Motil Cytoskeleton 39:172–190.

Menesini Chen MG, Chen JS, Levi-Montalcini R. 1978. Sympathetic nerve fibers ingrowth in the central nervous system of neonatal rodent upon intracerebral NGF injections. Arch Ital Biol 116:53–84.

Miki H, Yamaguchi S, Suetsugu S, Takenawa T. 2000. IRSp53 is an essential intermediate between Rac and WAVE in the regulation of membrane ruffling. Nature 408:732–735.

Ming GL, Song HJ, Berninger B, Holt CE, Tessier-Lavigne M, Poo MM. 1997. cAMP-dependent growth cone guidance by netrin-1. Neuron 19:1225–1235.

Mitchison T, Kirschner M. 1988. Cytoskeletal dynamics and nerve growth. Neuron 1:761–772.

Moore SW, Tessier-Lavigne M, Kennedy TE. 2007. Netrins and their receptors. Adv Exp Med Biol 621:17–31.

Morris MC, Depollier J, Mery J, Heitz F, Divita G. 2001. A peptide carrier for the delivery of biologically active proteins into mammalian cells. Nat Biotechnol 19:1173–1176.

Mouneimne G, DesMarais V, Sidani M, Scemes E, Wang W, Song X, Eddy R, et al. 2006. Spatial and temporal control of cofilin activity is required for directional sensing during chemotaxis. Curr Biol 16:2193–2205.

Mouneimne G, Soon L, DesMarais V, Sidani M, Song X, Yip SC, Ghosh M, et al. 2004. Phospholipase C and cofilin are required for carcinoma cell directionality in response to EGF stimulation. J Cell Biol 166:697–708.

Mullins RD, Heuser JA, Pollard TD. 1998. The interaction of Arp2/3 complex with actin: Nucleation, high affinity pointed end capping, and formation of branching networks of filaments. Proc Natl Acad Sci USA 95:6181–6186.

Nagata-Ohashi K, Ohta Y, Goto K, Chiba S, Mori R, Nishita M, Ohashi K, et al. 2004. A pathway of neuregulin-induced activation of cofilin-phosphatase Slingshot and cofilin in lamellipodia. J Cell Biol 165:465–471.

Nieuwkoop PD, Farber J. 1994. Normal Table of Xenopus Laevis (Daudin). New York: Garland.

Niwa R, Nagata-Ohashi K, Takeichi M, Mizuno K, Uemura T. 2002. Control of actin reorganization by Slingshot, a family of phosphatases that dephosphorylate ADF/cofilin. Cell 108:233–246.

O'Connor TP, Bentley D. 1993. Accumulation of actin in subsets of pioneer growth cone filopodia in response to neural and epithelial guidance cues in situ. J Cell Biol 123:935–948.

Ohta Y, Kousaka K, Nagata-Ohashi K, Ohashi K, Muramoto A, Shima Y, Niwa R, et al. 2003. Differential activities, subcellular distribution and tissue expression patterns of three members of Slingshot family phosphatases that dephosphorylate cofilin. Genes Cells 8:811–824.

Pak CW, Flynn KC, Bamburg JR. 2008. Actin-binding proteins take the reins in growth cones. Nat Rev Neurosci 9:136–147.

Patel TD, Jackman A, Rice FL, Kucera J, Snider WD. 2000. Development of sensory neurons in the absence of NGF/TrkA signaling in vivo. Neuron 25:345–357.

Pavlov D, Muhlrad A, Cooper J, Wear M, Reisler E. 2007. Actin filament severing by cofilin. J Mol Biol 265:1350–1358.

Piper M, Holt C. 2004. RNA translation in axons. Annu Rev Cell Dev Biol 20:505–523.

Pollard TD, Borisy GG. 2003. Cellular motility driven by assembly and disassembly of actin filaments. Cell 112:453–465.

Prins KW, Lowe DA, Ervasti JM. 2008. Skeletal muscle-specific ablation of gamma(cyto)-actin does not exacerbate the mdx phenotype. PloS One 3:e2419.

Quinn CC, Pfeil DS, Wadsworth WG. 2008. CED-10/Rac1 mediates axon guidance by regulating the asymmetric distribution of MIG-10/Lamellipodin. Curr Biol 18:808–813.

Ressad F, Didry D, Egile C, Pantaloni D, Carlier MF. 1999. Control of actin filament length and turnover by actin depolymerizing factor (ADF/cofilin) in the presence of capping proteins and ARP2/3 complex. J Biol Chem 274:20970–20976.

Ridley AJ, Paterson HF, Johnston CL, Diekmann D, Hall A. 1992. The small GTP-binding protein rac regulates growth factor-induced membrane ruffling. Cell 70:401–410.

Roche FK, Marsick BM, Letourneau PC. 2009. Protein synthesis in distal axons in not required for growth cone responses to guidance cues. J Neurosci 29:638–652.

Round J, Stein E. 2007. Netrin signaling leading to directed growth cone steering. Curr Opin Neurobiol 17:15–21.

Sabry JH, O'Connor TP, Evans L, Torolan-Raymond A, Kirschner M, Bently D. 1991. Microtubule behavior during guidance of pioneer neuron growth cones in situ. J Cell Biol 115:381–395.

Sarmiere PD, Bamburg JR. 2003. Regulation of the neuronal actin cytoskeleton by ADF/cofilin. J Neurobiol 58:103–117.

Schuman EM. 1999. Neurotrophin regulation of synaptic transmission. Curr Opin Neurobiol 9:105–109.

Seeley PJ, Greene LA. 1983. Short-latency local actions of nerve growth factor at the growth cone. Proc Natl Acad Sci USA 80:2789–2793.

Shaw AE, Minamide LS, Bill CL, Funk JD, Maiti S, Bamburg JR. 2004. Cross-reactivity of antibodies to actin-depolymerizing factor/cofilin family proteins and identification of the major epitope recognized by a mammalian actin-depolymerizing factor/cofilin antibody. Electrophoresis 25:2611–2620.

Shekarabi M, Moore SW, Tritsch NX, Morris SJ, Bouchard J-F, Kennedy TE. 2005. Deleted in colorectal cancer binding netrin-1 mediates cell substrate adhesion and recruits Cdc42. Rac1, Pak1 and N-WASP into an intracellular signaling complex that promotes growth cone expansion. J Neurosci 25:3132–3141.

Song HJ, Poo MM. 1999. Signal transduction underlying growth cone guidance by diffusible factors. Curr Opin Neurobiol 9:355–363.

Song H, Poo MM. 2001. The cell biology of neuronal navigation. Nat Cell Biol 3:E81–E88.

Strasser GA, Rahim NA, VanderWaal KE, Gertler FB, Lanier LM. 2004. Arp2/3 is a negative regulator of growth cone translocation. Neuron 43:81–94.

Suter DM, Forscher P. 1998. An emerging link between cytoskeletal dynamics and cell adhesion molecules in growth cone guidance. Curr Opin Neurobiol 8:106–116.

Svitkina TM, Borisy GG. 1999. Arp2/3 complex and actin depolymerizing factor/cofilin in dendritic organization and treadmilling of actin filament array in lamellipodia. J Cell Biol 145:1009–1026.

Tanaka E, Sabry J. 1995. Making the connection: Cytoskeletal rearrangements during growth cone guidance. Cell 83:171–176.

Tessier-Lavigne M, Goodman C. 1996. The molecular biology of axon guidance. Science 274:1123–1133.

Theriot JA, Mitchison TJ. 1991. Actin microfilament dynamics in locomoting cells. Nature 352:126–131.

Toshima J, Toshima JY, Takeuchi K, Mori R, Mizuno K. 2001. Cofilin phosphorylation and actin reorganization activities of testicular protein kinase 2 and its predominant expression in testicular Sertoli cells. J Biol Chem 276:31449–31458.

Van Troys M, Huyck L, Leyman S, Dhaese S, Vandekerkhove J, Ampe C. 2008. Ins and outs of ADF/cofilin activity and regulation. Eur J Cell Biol 87:649–667.

Weiner OD, Servant G, Welch MD, Mitchinson TJ, Sedat JW, Bourne JR. 1999. Spatial control of actin polymerization during neutrophil chemotaxis. Nat Cell Biol 1:75–81.

Wen Z, Han L, Bamburg JR, Shim S, Ming GL, Zheng JQ. 2007. BMP gradients steer nerve growth cones by a balancing act of LIM kinase and slingshot phosphatase on ADF/cofilin. J Cell Biol 178:107–119.

Wu KY, Hengst U, Cox LJ, Macosko EZ, Jeromin A, Urquhart ER, Jaffrey SR. 2005. Local translation of RhoA regulates growth cone collapse. Nature 436:1020–1024.

Yang N, Higuchi O, Ohashi K, Nagata K, Wada A, Kangawa K, Nishida E, et al. 1998. Cofilin phosphorylation by LIMK-kinase 1 and its role in Rac-mediated actin reorganization. Nature 393:809–812.

Yao J, Sasaki Y, Wen Z, Bassell GJ, Zheng JQ. 2006. An essential role for beta-actin mRNA localization and translation in Ca^{2+}-dependent growth cone guidance. Nat Neurosci 9:1265–1273.

Zebda N, Bernard O, Bailly M, Welti S, Lawrence DS, Condeelis JS. 2000. Phopshorylation of ADF/cofilin abolishes EGF-induced actin nucleation at the leading edge and subsequent lamellipod extension. J Cell Biol 151:1119–1128.

Zhou FQ, Cohan CS. 2003. How actin filaments and microtubules steer growth cones to their targets. J Neurobiol 58:84–89.

Zhou FQ, Zhou J, Dedhar S, Wu Y-H, Snider WD. 2004. NGF-induced axon growth is mediated by localized inactivation of GSK-3ß and functions of the microtubule plus end binding protein APC. Neuron 42:897–912.